

Predictions for the LHC heavy ion programme

Nicolas Borghini[†] and Urs Achim Wiedemann[‡]

[†] Fakultät für Physik, Universität Bielefeld, Postfach 100131, D-33501 Bielefeld, Germany

[‡] CERN, Department of Physics, Theory Division, CH-1211 Geneva 23, Switzerland

E-mail: borghini@physik.uni-bielefeld.de, Urs.Wiedemann@cern.ch

Abstract. Apparently universal trends have been observed in relativistic nucleus-nucleus collisions up to RHIC energies. Here, we review these trends and we discuss their agnostic extrapolation to heavy ion collisions at the LHC.

PACS numbers: 12.38.Mh, 25.75.Nq

Invited topical review for J. Phys. G: Nucl. Part. Phys.

1. Introduction

The main goal of ultra-relativistic heavy ion physics is to test the properties of matter, produced in nucleus-nucleus collisions at the highest energy densities accessible in the laboratory, and to develop an understanding of these properties from first principles of the fundamental theory of strong interactions, Quantum Chromodynamics (QCD). To this end, particle production in heavy ion collisions and its dependence on the formation of a dense system can be studied experimentally as a function of a large number of variables. These variables include the kinematic ones (such as centre-of-mass energy, transverse momentum and rapidity), as well as variables specific to heavy ion collisions, which typically control the size and shape of the collision region (such as the impact parameter or the nuclear number A of the colliding nuclei).

Over the last two decades, relativistic heavy ion collisions have been studied experimentally at increasingly higher centre-of-mass energies at the Brookhaven Alternating Gradient Synchrotron AGS ($\sqrt{s_{NN}} < 5$ GeV), the CERN Super Proton Synchrotron SPS ($\sqrt{s_{NN}} \leq 20$ GeV) and the Brookhaven Relativistic Heavy Ion Collider RHIC ($\sqrt{s_{NN}} \leq 200$ GeV). As discussed in this article, the data collected in these experimental campaigns display remarkable generic trends as a function of system size and kinematic variables.

The Large Hadron Collider LHC at CERN will study heavy ion collisions at a centre-of-mass energy $\sqrt{s_{NN}} = 5.5$ TeV, which is almost a factor 30 higher than the maximal collision energy at RHIC. There has been a lot of work in recent years on benchmarking model calculations of heavy ion collisions to RHIC data and extrapolating them to the higher LHC energies[‡]. The present topical review does not aim at such a comprehensive summary. Rather, the aim of this review is to identify the generic trends in the existing data and to discuss the consequences for our understanding of heavy ion collisions if these trends should persist or should fail to persist at the LHC. For those classes of measurements, where guidance from existing data is scarce (for instance for measurements at high- p_T or forward rapidity, where LHC is unique), we shall focus on generic features in the current model calculations, and discuss how they are expected to manifest themselves at the LHC.

We believe that the identification of generic trends in the data and their agnostic extrapolation to LHC energies may help to sharpen our view on what is expected at LHC energies and what constitutes a surprise. In addition, many of the generic trends listed in this article did not yet find a fully satisfactory explanation. If they persist at the LHC, this would indicate that they should not be discarded as mere numerical coincidences, but should find an explanation in a future, more complete theory.

[‡] A comprehensive update on these efforts will be given in the proceedings of a recent CERN Theory Institute workshop [1].

2. Multiplicity distributions

In $e^+e^- \rightarrow q\bar{q} \rightarrow X$, where the partons produced initially carry perturbatively high virtuality, main characteristics of the longitudinal and transverse multiplicity distributions can be understood quantitatively from the dynamics of the perturbative parton shower (see e.g. [2]), despite uncertainties in the modelling of hadronization. In contrast, in hadronic collisions, event multiplicities and multiplicity distributions are dominated by processes involving non-perturbatively small momentum transfers; there are many models but an understanding of multiplicity distributions based on first principles is missing. Even in proton-proton collisions, the extrapolation of the charged particle multiplicity per unit rapidity dN_{ch}/dy from the Tevatron ($\sqrt{s_{NN}} = 1.8$ TeV) to the LHC ($\sqrt{s_{NN}} = 14$ TeV) leads to results which vary by a factor 2 for models successful up to Tevatron energies [3]. For nucleus-nucleus collisions, the uncertainties in the predictions of minimum bias event multiplicities are of comparable magnitude. For instance, prior to the start-up of RHIC, model extrapolations of dN_{ch}/dy from the SPS centre-of-mass energy for Pb-Pb collisions ($\sqrt{s_{NN}} = 17$ GeV) to Au-Au collisions at RHIC ($\sqrt{s_{NN}} = 200$ GeV) varied by a factor 2 approximately [4, 5]. RHIC data lie at the lower end of the predicted range. This in turn has narrowed the range of predictions for the LHC.

The lack of a fundamental understanding of multiparticle production in hadronic collisions is in marked contrast to several characteristic features, which persist over many orders of magnitude in $\sqrt{s_{NN}}$ [6]:

- (i) Extended longitudinal scaling (limiting fragmentation [7]).

Pseudorapidity distributions[§], plotted in the rest frame of one of the colliding hadrons, fall on a universal, energy-independent limiting curve in the projectile fragmentation region. The region within which this limiting curve is valid, increases with energy, see figure 1. This is in contrast to the expectation that at high energies a boost-invariant plateau would develop around mid-rapidity.

- (ii) Factorization of $\sqrt{s_{NN}}$ and centrality/ A -dependence.

For all processes at a given centre-of-mass energy, the pseudorapidity distribution is the same basic distribution adjusted for the number of participants in the two colliding systems. The $\sqrt{s_{NN}}$ - and N_{part} -dependences of $dN_{\text{ch}}^{AA}/d\eta$ factorize.

The apparent universality of these observations motivates an agnostic extrapolation to the LHC: If A - A data at LHC follow the same limiting fragmentation curve and if the trapezoidal shape of pseudo-rapidity distributions persists, then one expects for $dN_{\text{ch}}^{\text{AA}}/d\eta$ at LHC the solid line in figure 1. This curve implies $dN_{\text{ch}}^{\text{PbPb}}/d\eta \sim 1100$.

[§] Pseudorapidity $\eta \equiv \tanh^{-1} p_l/p$ is for many purposes a good approximation of rapidity $y \equiv \tanh^{-1} p_l/E$. However, since multiplicity distributions are dominated by particles at small transverse momentum, there are visible differences: $dN_{\text{ch}}^{AA}/d\eta$ is of trapezoidal shape (see figure 1), while dN_{ch}^{AA}/dy is of Gaussian shape. So, figure 1 does *not* imply a rapidity plateau. For A - A collisions, multiplying $dN/d\eta$ at $\eta = 0$ by the conversion factor ≈ 1.1 turns out to be a good estimate for dN/dy at $y = 0$.

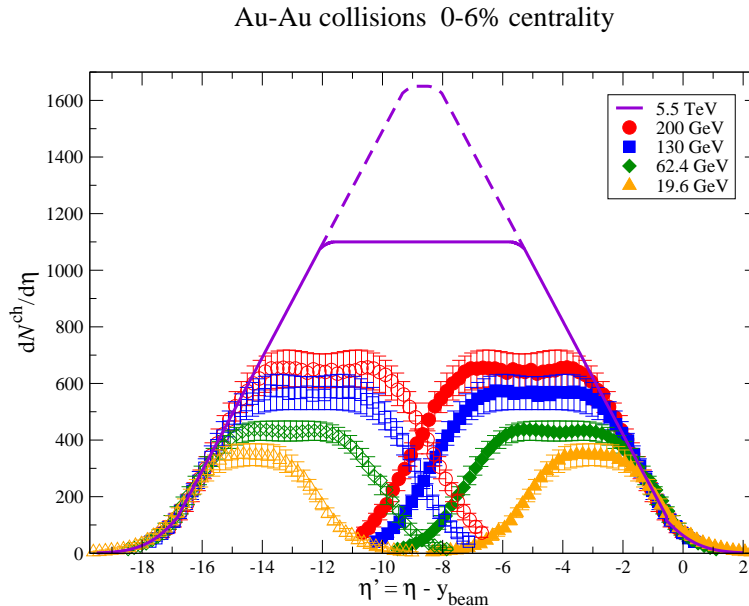


Figure 1. Pseudorapidity distribution of charged particle production in Au-Au collisions at different centre-of-mass energies. Data are plotted in the rest frame of one of the colliding nuclei (full symbols), and mirrored at LHC mid-rapidity (open symbols). Agnostic extrapolations to the LHC are based on assuming limiting fragmentation and i) the saturation ansatz (1) (dashed line), or ii) a self-similar trapezoidal shape of the multiplicity distribution (solid line). Data from [8, 9].

More generally, the persistence of extended longitudinal scaling in the high energy limit implies that at mid-rapidity, dN/dy can grow at most logarithmically with \sqrt{s} , except if there is a novel mechanism due to which the curvature of dN/dy changes its sign *twice* between $y = 0$ and the fragmentation region.

Essentially all models of multiplicity distributions predict a power-law increase with $\sqrt{s_{NN}}$. This is a rather generic consequence of perturbative particle production mechanisms, which become more important with increasing \sqrt{s} . However, the power-law dependence of naive perturbative implementations is too strong to be reconciled with RHIC data — this is arguably the main lesson learnt from the failure of many models at RHIC. Saturation models have received much attention recently, since they offer a fundamental reason for the very weak \sqrt{s} -dependence of event multiplicities, namely the taming of the perturbative rise due to density-dependent non-linear parton evolution. Still, saturation models assume that multiplicity distributions at ultra-relativistic energies are calculable within perturbation theory, since they are governed by a perturbatively high, \sqrt{s} - and A -dependent momentum (saturation) scale $Q_{\text{sat},A}^2 \propto \sqrt{s}^\lambda$. They predict essentially, that multiplicities at mid-rapidity rise $\propto Q_{\text{sat},A}^2$ times transverse area. This leads e.g. to the pocket formula [10]

$$\frac{2}{N_{\text{part}}} \left. \frac{dN_{\text{ch}}^{AA}}{d\eta} \right|_{\eta \sim 0} = N_0 \sqrt{s_{NN} [\text{in GeV}]}^\lambda N_{\text{part}}^{\frac{1-\delta}{3\delta}}. \quad (1)$$

Here $N_0 = 0.47$ is fixed by fitting to RHIC multiplicity distributions. The factors

$\lambda = 0.288$ and $\delta = 0.8$ are constrained by fitting data on eA inelastic scattering. In this sense, the \sqrt{s} - and A -dependences of (1) are predicted. The pocket formula (1) provides an explicit realization of the factorization property (ii) stated above, and accounts satisfactorily for the \sqrt{s} - and A -dependences of charged multiplicity distributions from SPS to maximal RHIC energies [10]. For central Pb-Pb collisions at the LHC, equation (1) leads to $dN_{\text{PbPb}}^{\text{ch}}/d\eta \sim 1650$, which corresponds to the maximum of the dashed line in figure 1. An alternative model implementation of saturation physics ideas arrives at $dN_{\text{PbPb}}^{\text{ch}}/d\eta \sim 2200$ [11]. A similar value is also predicted by the EKRT final state saturation model [12], which arrives at a $\sqrt{s_{NN}}^{0.38}$ -dependence of the charged multiplicity at mid-rapidity. To arrive at a $\ln \sqrt{s_{NN}}$ -dependence in such schemes, one would have to invoke a mechanism, which amputates brutally the power-law tail in the spectrum for $p_T^2 > Q_s^2$ (see e.g. the discussion of D. Kharzeev in reference [1]).

A complete list of model predictions is beyond the scope of this article. We emphasize, however, that none of these predictions can be reconciled with the assumption that the so-far universal extended longitudinal scaling persists at LHC energies. As seen from figure 1, a distribution matching $dN_{\text{PbPb}}^{\text{ch}}/d\eta \sim 2200$ at mid-rapidity has to fall off significantly steeper than what is consistent with limiting fragmentation. Also, the prediction $dN_{\text{PbPb}}^{\text{ch}}/d\eta \sim 1650$, while being close to the maximum of what is consistent with limiting fragmentation, appears to deviate characteristically from the trapezoidal shape of all pseudo-rapidity distributions of charged multiplicity measured so far.

To summarize and generalize this discussion: Either, the apparently universal “structure” seen in multiparticle production data at lower energies [6] is violated at the LHC. Then, this violation is likely to provide highly discriminatory constraints on the dynamics underlying multiparticle production. Or, the naive extrapolations of this structure to the LHC are confirmed. Then, the central dynamical ideas advocated as explanations for the tamed growth of multiplicities up to RHIC energies will have to be revisited. So, starting with the first day of operation, data from the LHC are likely to have profound consequences for our understanding of the matter produced in nucleus-nucleus collisions at the LHC *and* at RHIC.

3. Hadrochemistry

The relative abundance of identified hadron species in heavy ion collisions follows a statistical (“thermal”) distribution pattern over a very broad energy range from SIS/GSI ($\sqrt{s_{NN}} \approx 2$ GeV) up to RHIC ($\sqrt{s_{NN}} = 200$ GeV) [13]. For particle species, for which global constraints (such as total charge or flavour conservation) are statistically unimportant because of sufficiently large event multiplicities, particle ratios are well described by the grand canonical ensemble of a hadron resonance gas. The only parameters of this model are the temperature T at chemical decoupling, and the baryon chemical potential μ_B . Fits to particle ratios reveal a characteristic $\sqrt{s_{NN}}$ -dependence of these parameters, see figure 2. The baryon chemical potential decreases by almost an

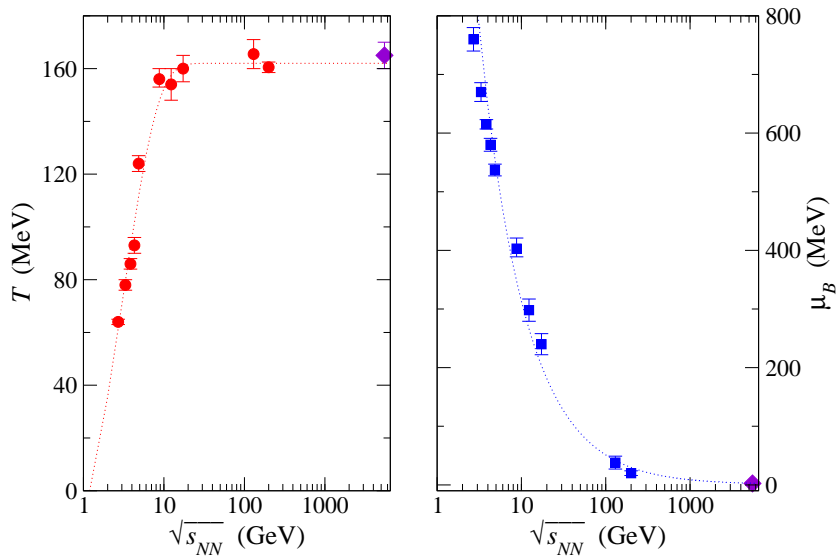


Figure 2. Thermal model fits at mid-rapidity of the hadrochemical freeze-out temperature T and the baryochemical potential μ_B as a function of the centre-of-mass energy $\sqrt{s_{NN}}$. Data points up to RHIC energies are taken from reference [14]. Data points at $\sqrt{s_{NN}} = 5.5$ TeV are based on simple extrapolations of the observed tendency.

order of magnitude from $\mu_B \sim 250$ MeV at the SPS to $\mu_B \sim 20$ -40 MeV at RHIC and is generally assumed to be very small ($\mu_B \ll 10$ MeV) at LHC mid-rapidity. This reflects the expectation that due to the large difference between projectile and mid-rapidity at the LHC, the mid-rapidity region is almost net-baryon free. The chemical decoupling temperature approaches a $\sqrt{s_{NN}}$ -independent limiting temperature $T \simeq 160 - 170$ MeV, which seems to be almost reached at RHIC and which is expected to persist at the LHC. These agnostic extrapolations to LHC energies have been used to predict the ratios of more than twenty hadron species, and there are computer codes implementing these model assumptions [15–18]. Early works on hadronic abundances used a strangeness saturation parameter [19] to account for enhanced strangeness production with increasing $\sqrt{s_{NN}}$. This followed the idea that with increasing $\sqrt{s_{NN}}$ a gluon-rich initial system is formed, which is more efficient in producing strangeness. In contrast, the above-mentioned models do not fix the strangeness content with an additional parameter. These models explain strangeness increase by a *suppression* of strange particles in low-multiplicity systems created at lower $\sqrt{s_{NN}}$. This suppression is due to exact conservation laws, whose implementation leads to deviations from the grand-canonical limit [13]. The resulting canonical suppression factors are known analytically.

At RHIC and at the LHC, canonical suppression is unimportant for strangeness, which is produced abundantly. On the other hand, canonical suppression is important for open charm [20] and bottom production at the LHC. In this general sense, charm and bottom are likely to play at collider energies a similar role as strangeness played

during the fixed-target era of heavy-ion physics. There is, however, one important difference: because of their large mass and small production cross section at thermal energies, the thermal production of charm and bottom quarks is disfavoured. Thus, except for the very first proposals of thermal charm production [21], models assume normally a production of heavy-flavoured quarks at perturbative rates, followed by a hadrochemical distribution of heavy-flavoured resonances according to the statistical model of hadroproduction [20]. In this approach, the centrality dependence of charm-flavoured particle ratios tests the transition from a canonical to a grand-canonical description.

The models discussed so far implement the idea of statistical hadronization, but they do *not* specify the dynamics leading to the hadronic final state. In particular, although the hadrochemical freeze-out temperature and baryochemical potential shown in figure 2 match within errors the QCD phase-space boundary determined in lattice QCD, the question whether this agreement implies the existence of dynamical thermalization processes lacks a more detailed support [22]. We conclude this section by listing three possibilities of how heavy-ion collisions at the LHC may help to elucidate the microscopic dynamics underlying hadronic abundances: First, it has been conjectured that charmonium production at the LHC is strongly enhanced above the perturbatively expected rates due to the recombination of c and \bar{c} quarks originating in distinct hard partonic interactions [23]. Establishing such a novel charmonium production mechanism could provide a strong indication that thermalization processes affect hadrochemical distributions. This is so, since transport of exogamous c - and \bar{c} -partners is likely to be necessary to make their coalescence possible. Second, we mention in passing a proposal that the abundances of strange hadrons could exceed significantly grand-canonical predictions. This is seen in models in which a *sudden* hadronization of an equilibrated plasma leads to strangeness over-saturation in the hadronic phase [24]. While arguably speculative, this example illustrates that the extrapolation of (standard) statistical model predictions to the LHC can serve as a powerful baseline on top of which novel dynamical effects may be established. Third, the masses and widths of the resonances entering the statistical operator of a resonance gas model may receive significant medium-modifications. This may lead to deviations of some broad resonances (such as ρ -mesons) from the grand canonical ensemble. While not specific for the LHC, it is likely that any confirmation and extended systematics of such deviations will provide constraints on the in-medium dynamics of hadronic resonances near freeze-out.

4. Transverse-momentum spectra at low p_T

The transverse momentum dependence of identified single inclusive hadron spectra has been studied in heavy ion collisions from SIS/GSI up to RHIC energies. Here, we follow the common practice of discussing these spectra as a function of their transverse mass $m_T = \sqrt{m^2 + p_T^2}$, rather than their transverse momentum. The m_T -distributions are commonly characterized by a mono-exponential fit $dN/dm_T \propto m_T^{3/2} \exp[-m_T/T_{\text{inv}}]$ [25],

where the inverse-slope parameter T_{inv} characterizes the steepness of the distributions. The fit value T_{inv} can depend on the m_T -range over which the fit is performed, but despite the ensuing uncertainties, the following generic features can be stated:

(i) Linear mass-dependence of T_{inv} .

At given $\sqrt{s_{NN}}$, the inverse-slope parameters of pions, kaons, and protons increase *approximately linearly* with the particle rest mass. In particular $T_{\text{inv},\pi^\pm} < T_{\text{inv},K^\pm} < T_{\text{inv},p}$. The hadrons, which do not follow this systematics, such as the multistrange Ξ , the Ω or the J/Ψ , show roughly the same value T_{inv} . A seemingly common denominator of these latter hadrons is their relatively small interaction cross sections with the expected constituents of the medium [26,27].

(ii) Increase of T_{inv} with $\sqrt{s_{NN}}$.

The spectra become flatter with increasing $\sqrt{s_{NN}}$, so the inverse slope parameter T_{inv} increases. Also, the mass-dependence of T_{inv} for pions, kaons and protons increases with $\sqrt{s_{NN}}$ [26].

The inverse-slope parameter T_{inv} has been interpreted as a blue-shifted temperature, resulting from a combination of thermal emission from a source of temperature $T_{\text{f.o.}}$ at freeze-out, and the collective motion with average transverse velocity $\langle\beta_T\rangle$ of this particle emitting source. While $T_{\text{f.o.}}$ and $\langle\beta_T\rangle$ are difficult to disentangle on the basis of single inclusive spectra alone, two-particle correlations may be used to separate both contributions [28]. The increase of T_{inv} with particle rest mass [point (i)] is consistent with the interpretation of T_{inv} as a blue-shifted temperature [25,29], if the particles decouple at the time of freeze-out. On the other hand, particles which decouple earlier due to their smaller cross sections would acquire less radial flow, and thus have a smaller T_{inv} . In this radial-flow picture, the growing difference between inverse-slope parameters as $\sqrt{s_{NN}}$ increases [point (ii)] is ascribed to the growth in the average transverse velocity $\langle\beta_T\rangle$.

The above features emerge naturally in fluid-dynamics models without [30,31] or with [32] viscous corrections. We are not aware of full fluid-dynamic studies of these spectra at LHC energy. However, there are extrapolations of the fit parameters $T_{\text{f.o.}}$ and $\langle\beta_T\rangle$, extracted from the approximately exponential m_T -spectra [26]. In these studies, the kinetic freeze-out temperature saturates at a value $T_{\text{f.o.}} \approx 120$ MeV at SPS energy, which may be expected to persist up to the LHC. The parameter $\langle\beta_T\rangle$ is found to increase with $\sqrt{s_{NN}}$; it reaches $\langle\beta_T\rangle \approx 0.55$ at RHIC, but it remains unclear whether this increase is smooth [26].

The statements made here are obtained within a blast-wave model [26,29] or within a fluid-dynamic picture supporting such a model. They generally indicate an increase of T_{inv} with $\sqrt{s_{NN}}$. Here, the real physical issue is to assess whether it is really a collective hydrodynamic mechanism, which determines the energy-dependence of T_{inv} . Since the slope of spectra evolves significantly with $\sqrt{s_{NN}}$ also for more elementary proton-proton collisions, in which flow is either absent or at least different, it is not straightforward to disentangle flow effects from other mechanisms. This makes quantitative comparisons

difficult and leads to a lack of precision in extrapolations to the LHC. We now turn to the azimuthal dependence of single inclusive transverse momentum spectra, where these difficulties appear to be less severe.

5. Azimuthal anisotropy in low- p_T particle production

In non-central collisions, the impact parameter selects a preferred direction in the transverse plane, breaking the rotational symmetry around the beam axis. Consequently, observables can depend on azimuth, measured with respect to the reaction plane spanned by the impact parameter and the beam direction. The azimuthally-dependent effect most widely studied both experimentally, over the whole range of available collision energies, and theoretically, is the azimuthal anisotropy in particle production, often referred to as “anisotropic (transverse) flow” [31]. A non-vanishing anisotropic flow exists only if the particles measured in the final state depend not only on the physical conditions realized locally at their production point, but if particle production does also depend on the global event geometry. In a relativistic local theory, this non-local information can only emerge as a collective effect, requiring interactions between many degrees of freedom, localized at different points in the collision region. In this general sense, anisotropic flow is a particularly unambiguous and strong manifestation of collective dynamics in heavy-ion collisions. Here, we discuss its features for hadrons at low- p_T .

Azimuthal anisotropies in particle production are most conveniently characterized by performing a Fourier expansion of the single-particle distribution

$$\frac{dN}{d^2\mathbf{p}_t dy} = \frac{1}{2\pi} \frac{dN}{p_T dp_T dy} [1 + 2v_1 \cos(\phi - \Phi_R) + 2v_2 \cos 2(\phi - \Phi_R) + \dots], \quad (2)$$

where Φ_R denotes the azimuth (in the laboratory frame) of the reaction plane. The coefficients $v_n = \langle \cos n(\phi - \Phi_R) \rangle$, where angular brackets denote an average over many particles and events, quantify the asymmetry. These coefficients are studied at all available energies as a function of transverse momentum, (pseudo)rapidity, centrality of the collision and for various identified particle species.

“Elliptic flow”, the second Fourier coefficient v_2 is the best studied one. A positive (resp. negative) value of v_2 indicates an excess of particle production in (resp. orthogonal to) the reaction plane. The dependence of v_2 on centre-of-mass energy is known over three orders of magnitude, see figure 3. It can be understood qualitatively in terms of the following simple picture of a collective dynamics: At $\sqrt{s_{NN}} < 2$ GeV, the incoming nuclei transfer angular momentum to the nuclear matter in the overlap zone. The fast-rotating “compound nucleus” thus formed emits fragments, which lie preferentially in the reaction plane ($v_2 > 0$). As the centre-of-mass energy increases, the nuclear matter in the almond-shaped overlap region of the incoming nuclei is increasingly compressed in the collision. However, the parts of the nuclei that lie outside this overlap region (“spectators”) block the way for the compressed matter to expand within the reaction plane. They *squeeze-out* the compressed matter orthogonal to the reaction plane

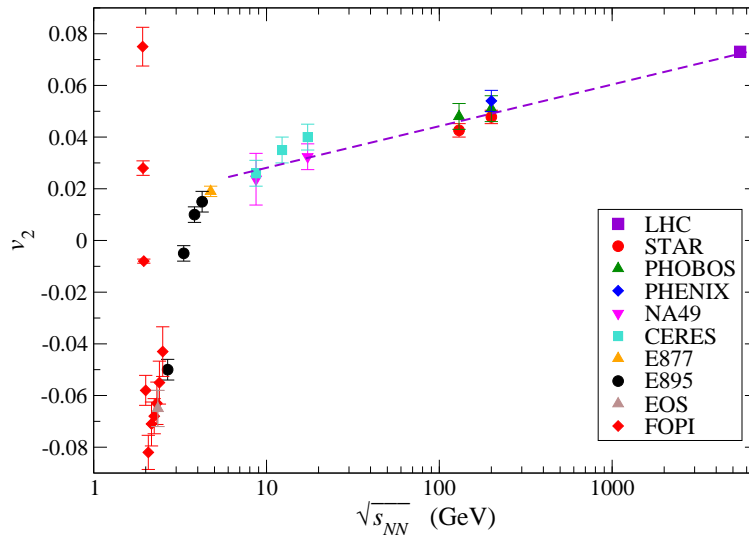


Figure 3. $\sqrt{s_{NN}}$ -excitation function of $v_2(y=0)$ in mid-central collisions. Data are taken from the compilation in reference [33].

($v_2 < 0$). Further increasing $\sqrt{s_{NN}}$, the spectators are then fast enough to free the way, leaving behind at mid-rapidity an almond-shaped azimuthally asymmetric region of dense QCD matter. This spatial asymmetry implies unequal pressure gradients in the transverse plane, with a larger gradient in the reaction plane (“in-plane”) than perpendicular to it. As a consequence of the subsequent multiple interaction between many degrees of freedom, this spatial asymmetry leads to an anisotropy in momentum space: the final particle transverse momenta are more likely to be in-plane than “out-of-plane”, hence $v_2 > 0$, as predicted in [34].

The momentum space asymmetries measured at collider energies are relatively large. Since the prefactor of the cosine term in equation (2) is $2v_2$, a p_T -averaged value $v_2 = 0.05$ corresponds to a 20% variation of the average particle yield as a function of the angle with respect to the reaction plane. At high p_T , where second harmonics at RHIC approached values as large as $v_2 = 0.2$, there are more than twice the number of particles emitted in the reaction plane than out-of-plane. Elliptic flow is an abundant and very strong manifestation of collectivity, which shows remarkable generic trends:

- (i) The p_T -integrated $v_2(\eta)$ shows extended longitudinal scaling [35].

In contrast to $dN/d\eta$, $v_2(\eta)$ is not trapezoidal but triangular, see figure 4||. As seen clearly from figure 4, longitudinal scaling of p_T -integrated v_2 persists up to mid-rapidity.

- (ii) The p_T -shape of the charged-hadron v_2 has a characteristic breaking point.

At transverse momenta below $p_T \simeq 2$ GeV/c, where data are known from SPS and RHIC, v_2 is found to have an approximately linear rise with p_T . Around $p_T \simeq 2$ GeV/c, this rise levels off rather abruptly. The energy-dependence of this

|| The p_T -averaged value of v_2 is dominated by values of the transverse momentum close to $\langle p_T \rangle$, so that $v_2(\eta)$ and $v_2(y)$ are similar, in contrast to $dN/d\eta$ and dN/dy .

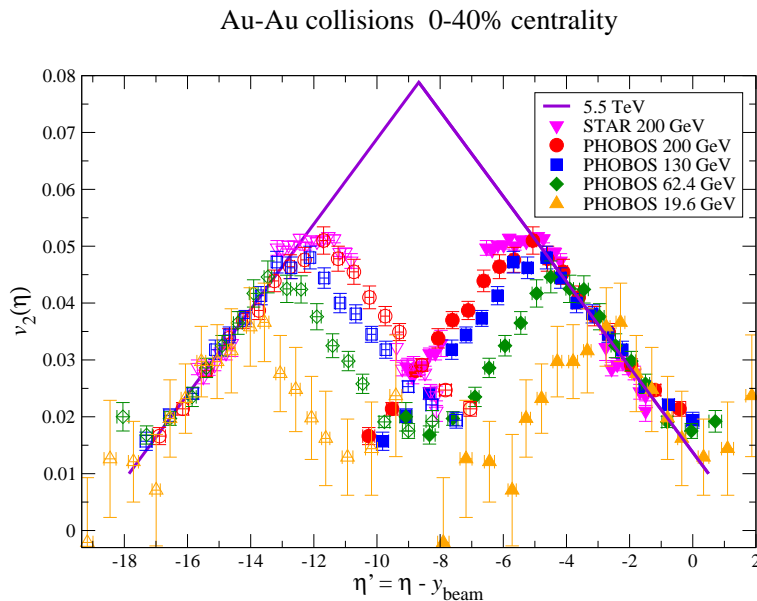


Figure 4. The elliptic flow v_2 , averaged over centrality (0%-40%), at various collision energies. Data (full symbols) from PHOBOS [35] and STAR [36] are plotted as a function of $\eta - y_{\text{beam}}$ and reflected (open symbols) across the LHC $-y_{\text{beam}}$ value.

p_T -shape is not fully clarified: At low p_T , the slope of $v_2(p_T)$ was reported to rise either slightly [37] or significantly [38] across SPS and RHIC energies. Also, it was reported [38] that the slope of $v_2(p_T)$ saturates at RHIC energies and is essentially constant between $\sqrt{s_{NN}} = 62.4$ GeV and 200 GeV. In this case, the increase of the p_T -averaged v_2 would be entirely due to the increase in the mean transverse momentum of particles.

- (iii) The p_T -dependent v_2 of identified hadrons shows mass-ordering at small p_T and displays a constituent-quark counting rule at intermediate p_T .

For a fixed, sufficiently low transverse momentum, SPS and RHIC data show generically that $v_2(p_T)$ decreases with increasing mass of the particle species. Above a critical $p_T \sim 1.5$ GeV/ c , mass-ordering ceases to be valid and $v_2(p_T)$ follows to a good approximation a simple quark counting rule, namely that $v_2(p_T/n_q)/n_q$ is roughly independent of the particle species [39].

What are the implications if these trends persist or do not persist at the LHC?

First, if longitudinal scaling of v_2 persists, then $v_2(\eta)$ grows proportional to $\ln \sqrt{s_{NN}}$. In this case, one expects $v_2(\eta = 0) \simeq 0.075$ for Pb-Pb collisions in mid-central collisions. This follows from the extrapolations, shown in figures 3 and 4. To the best of our knowledge, neither the triangular shape of the rapidity dependence of v_2 , nor the approximately linear $\ln \sqrt{s_{NN}}$ -dependence emerges as a natural consequence of existing dynamical models. In particular, extrapolating models of ideal hydrodynamics from RHIC to the LHC, one arrives at values not exceeding $v_2(\eta = 0) \simeq 0.06$ for event multiplicities shown in figure 1 [30]. Also, the proportionality $v_2(y) \propto dN/dy$ does not hold in models presupposing local equilibrium (i.e. the formation of an almost perfect

fluid). If the matter produced at RHIC mid-rapidity is in local equilibrium, then one expects at the LHC deviations from the triangular shape of $v_2(\eta)$ in an extended region $-3 \lesssim y \lesssim 3$, around mid-rapidity¶. In summary: extrapolations to the LHC of the main dynamical mechanism advocated to underlie elliptic flow at RHIC (namely perfect fluid dynamics) are at odds with extrapolations to the LHC of the generic trends observed in elliptic flow measurements up to RHIC energy. As a consequence, establishing whether these trends persist at the LHC provides a novel independent test for our understanding of the properties of matter at the LHC *and* at RHIC.

Second, comparing measurements of $v_2(p_T)$ from LHC and RHIC at low p_T will finally allow us to establish to what extent the p_T -slope of $v_2(p_T)$ changes with $\sqrt{s_{NN}}$. This is of interest, since a $\sqrt{s_{NN}}$ -independent slope of $v_2(p_T)$ would imply e.g. that the increase of the p_T -integrated $v_2(\eta)$ with $\sqrt{s_{NN}}$ arises solely from the increase of the average transverse momentum. Existing dynamical models of v_2 do not invoke the increase of the rms transverse momentum $\sqrt{\langle p_T^2 \rangle}$ with $\sqrt{s_{NN}}$ observed in hadronic collisions; so, establishing a major role of $\sqrt{\langle p_T^2 \rangle}$ in v_2 may prompt significant revision in our interpretation of elliptic flow. Moreover, LHC data for $v_2(p_T)$ at intermediate p_T will test to what extent the breaking point of $v_2(p_T)$ depends on centre-of-mass energy, collision centrality, or choice of nuclei, while existing RHIC data hint at a very small sensitivity on these [42]. In the current discussion of RHIC data, one emphasizes that the approximately linear increase of $v_2(p_T)$ at low p_T is consistent with the transverse expansion of an almost perfect liquid [31], while the breaking point in $v_2(p_T)$ arises from the rather abrupt onset of dissipative effects at higher p_T [43]. However, transport models and dissipative hydrodynamics [43] can account for the linear increase of $v_2(p_T)$ at small p_T as well, if initial conditions are chosen appropriately, and a detailed understanding of the dynamical origin of the breaking point is missing and may profit from knowledge about its $\sqrt{s_{NN}}$ -dependence.

Third, mass-ordered $v_2(p_T)$ at mid-rapidity are predicted in transport approaches [44,45] as well as in hydrodynamical models [30,31], but details of the predicted mass hierarchy vary between models. For instance, two different ideal-fluid dynamics approaches predict scaling laws with different variables: the decoupling of all particle species from the same collective-flow field is argued in reference [46] to lead to a common $v_2(p_T/m)$ for all hadrons; while in the Buda-Lund framework [47] a scaling of $v_2(p_T)$ with the square of the transverse rapidity $y_T \equiv \frac{1}{2} \ln[(m_T + p_T)/(m_T - p_T)]$ is predicted. So, while mass ordering of $v_2(p_T)$ for light hadrons is expected to persist qualitatively, its quantitative manifestation may help to differentiate between models of the collision dynamics.

Moreover, at the LHC, the elliptic-flow parameters $v_2(p_T)$ of D - and B -mesons will provide yet another test of the mass-ordering of v_2 . Quantitative comparison to predictions of dynamical approaches — be it fluid dynamics, a Langevin description, or a transport model — have been argued to give insight on the possible thermalization [48]

¶ However, in models which presuppose incomplete local equilibration [40,41], one finds $v_2(y) \propto dN/dy$, thus accounting for the triangular shape of $v_2(\eta)$.

of heavy quarks, in particular their mean free path [49], and their hadronization mechanism [50, 51]. Quite generally, heavy quarks in equilibrium have a larger $v_2(p_T)$ than non-equilibrated ones; and the corresponding mesons have larger elliptic-flow values if they form through coalescence (involving a light quark) than if they come from heavy-quark fragmentation.

Mass-ordering persists essentially up to the breaking point in the p_T -shape. Above this point and up to $\approx 5\text{--}6$ GeV/ c , a quark-counting rule was observed at RHIC for light hadrons, defining a region of intermediate transverse momenta. (New n_q -scaling rules at low transverse momentum were also recently reported at RHIC [42, 52], which to our knowledge have no theoretical explanation in the existing literature.) The persistence of such rules at LHC would constrain dynamical models, especially those covering both the low- and intermediate- p_T regions.

We now turn to the centrality dependence of v_2 . It has been suggested to classify finite impact-parameter collisions for nuclei of different size in terms of the surface S of the transverse overlap region and the eccentricity ϵ of this surface. (We note that fluctuations [53, 54] and uncertainties in the initial conditions [55, 56] make the specification of ϵ and S somewhat model-dependent.) One observes that data of $v_2(y=0)/\epsilon$ from AGS to RHIC energy show an apparently universal, linear dependence if plotted against $(1/S)dN^{\text{ch}}/dy$ (see e.g. figure 25 in reference [57] or figure 15 in reference [58]). Modelling the matter produced in heavy ion collisions in terms of a perfect fluid, one finds that the above-mentioned linear dependence levels off above values of $(1/S)dN^{\text{ch}}/dy$ corresponding to central RHIC energies. Thus, as in our discussion of several other classes of measurements, a naive extrapolation of these data on centrality from RHIC to LHC is at odds with a naive extension of the main dynamical explanation advocated to underlie elliptic flow v_2 . On the other hand, there are models which may account for a further increase of v_2/ϵ due to non-equilibrium phenomena in the initial state [41], or due to a change in the relative contributions of hadronic and partonic rescattering effects as a function of $\sqrt{s_{NN}}$ [59], or due to a significant change in initial conditions [60].

The second most studied flow harmonic is v_1 , “directed flow”, which quantifies the average momentum acquired by the particles along the impact-parameter direction. Two generic trends can be identified in existing data:

- (i) The p_T -integrated $v_1(y)$ is linear around mid-rapidity.

At mid-rapidity, v_1 vanishes by symmetry in collisions between identical nuclei. A linear increase of $v_1(y)$ around $y = 0$ is observed across AGS and SPS energies. The slope dv_1/dy decreases with increasing beam energy.

- (ii) The p_T -integrated $v_1(\eta)$ shows extended longitudinal scaling [61].

Above SPS energy, one finds that $v_1(\eta)$ is positive in the “projectile” ($\eta > 0$) fragmentation region⁺, then becomes negative for $\eta \lesssim y_{\text{beam}}$, reaches a minimum

⁺ This is a choice, inherited from fixed-target studies at lower energies, where the bounce of the projectile off the target is taken to define the positive direction. The absolute sign of v_1 is not

for $-2 \lesssim \eta - y_{\text{beam}} \lesssim -1$, and increases.

The requirement that v_1 be zero at midrapidity implies either a breakdown of the longitudinal-scaling property, or that $v_1(\eta)$ vanishes in an extended region around $y = 0$ (so that the slope dv_1/dy is also zero), the size of which increases with beam energy. In either case, the p_T -integrated $v_1(y)$ at LHC will be smaller in absolute value than 0.01 up to rapidities $y \approx 4 - 5$. A deviation from this expectation would indicate a physics effect that manifestly breaks Bjorken boost-invariance and which becomes more pronounced at higher $\sqrt{s_{NN}}$. We are not aware of any suggestion of such an effect at these energies. Thus, testing a non-trivial dependence of v_1 at LHC and extending the RHIC systematics is likely to require measurements at far forward rapidity, which are experimentally challenging.

We finally comment on the fourth anisotropic-flow harmonic v_4 . It has been argued that at given transverse momentum and rapidity, $v_4(p_T, y) \geq \frac{1}{2}v_2(p_T, y)^2$ [41, 46], the lower bound being attained if and only if the matter expands like a perfect fluid at the time when anisotropic flow develops. At RHIC, one has reported $v_4/v_2^2 \simeq 1.2$ [62]. If one takes this number as an indication of incomplete equilibration, and if one assumes that equilibration mechanisms are more efficient at the LHC, one predicts $0.5 < v_4/v_2^2 < 1.2$ at the LHC. Without such assumptions, one still observes that both RHIC data and model calculations lead us to expect a value of v_4/v_2^2 of order unity.

6. Femtoscopy

The header *femtoscopy* summarizes a class of measurements that give access to the spatio-temporal extension and collective dynamics of the matter produced in heavy-ion collisions [63]. This includes in particular identical two-particle momentum correlations $C(\mathbf{K}, \mathbf{q})$ of relative pair momentum \mathbf{q} and average pair momentum \mathbf{K} . These are often analysed in the Bertsch-Pratt parametrization

$$C(\mathbf{K}, \mathbf{q}) = 1 + \lambda \exp \left[\sum_{i,j=\text{o},\text{s},\text{l}} R_{ij}(\mathbf{K}_\perp, K_L) q_i q_j \right]. \quad (3)$$

Here, the indices i, j label a Cartesian coordinate system with axes pointing along the *longitudinal* beam direction (*longitudinal* or “l”), parallel to the transverse pair momentum \mathbf{K}_\perp (*out* or “o”) and the remaining (*side* or “s”) one. The radius parameters $R_{ij}(\mathbf{K}_\perp, K_L)$ combine information about the spatial and temporal extension of the particle-emitting source at freeze-out. They do not measure the extension of the entire collision region, but they measure the generally smaller “homogeneity regions”, i.e. the part of the source radiating particle pairs with pair momentum (\mathbf{K}_\perp, K_L) . Data of these HBT radii, taken at the SPS and RHIC, display several generic trends:

- (i) Almost linear scaling with $(dN_{\text{ch}}/d\eta)^{1/3}$.

As seen in figure 5, the diagonal radius parameters in the out-, side-, and measurable, only its changes in sign are.

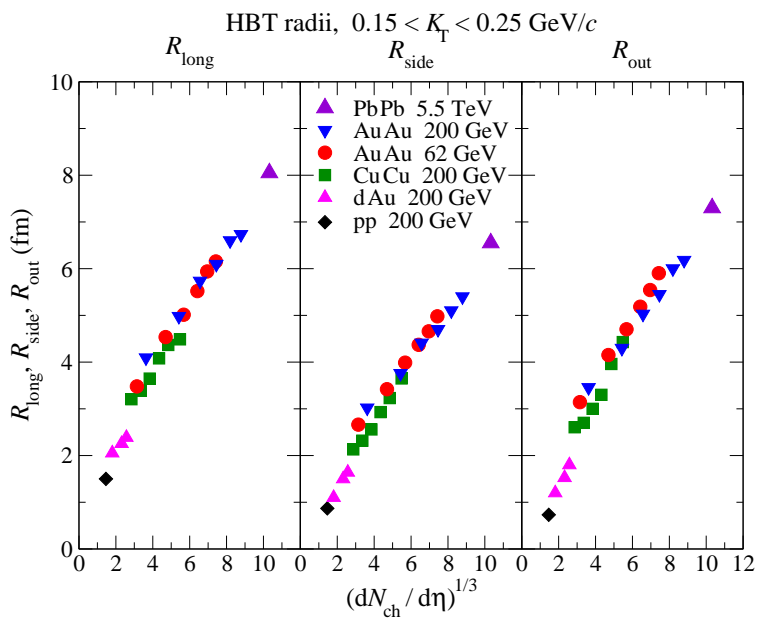


Figure 5. The diagonal HBT radius parameters R_l , R_s and R_o at mid-rapidity plotted versus event multiplicity for different centre-of-mass energies, including an extrapolation to LHC. Data from the STAR collaboration taken from reference [64]. Except for the 200 GeV Au-Au results, all data are preliminary, but consistent with previously observed trends [63].

longitudinal directions scale approximately linearly with the third root of the charged particle multiplicity per unit rapidity. The entire $\sqrt{s_{NN}}$ -dependence appears to arise via the dependence on $(dN_{ch}/d\eta)^{1/3}$.

(ii) Universal m_T -dependence.

Values for the HBT radius parameters of different particle species fall on a universal curve if plotted versus transverse mass, $m_T = \sqrt{m^2 + K_T^2}$. In particular, the ansatz

$$R_i(K_T) \simeq c_i \frac{1}{m_T^{\alpha_i}}, \quad (4)$$

provides a fair description of the universal m_T -dependence. Here, the parameters α_i and c_i take the same universal values for all hadron species. Fit values of α_i are ~ 0.5 , albeit with large variations.

(iii) $R_o^2 \simeq R_s^2$.

The three diagonal radius parameters differ in size, but this difference is small compared to their absolute value. In particular, $R_o^2 \simeq R_s^2$.

The extrapolation of the linear-scaling trend (i) from RHIC to the LHC leads to values for the HBT radius parameters that exceed significantly those measured previously, see figure 5. For instance, one finds $R_l(150 \text{ MeV} < K_T < 250 \text{ MeV}) \simeq 8 \text{ fm}$ for $dN_{ch}/d\eta = 1100$, and even larger values for larger event multiplicities. For central collisions at mid-rapidity, the off-diagonal radius parameters R_{ij} vanish by symmetry, and the product $V = R_l R_s R_o$ provides a working definition of the spatial volume of the

homogeneity region. The linear increase of all three HBT radii with $(dN_{\text{ch}}/d\eta)^{1/3}$ is then consistent with the statement, that hadrons freeze-out from the collision system at an universal phase-space density [65]. Changes in hadrochemical composition, transverse flow or temperature gradients may lead to deviations from this freeze-out criterion at universal phase-space density [66]. In particular, an increase of the fraction of baryons ($p + \bar{p} +$ higher resonances) at fixed density leads to an increase of HBT radius parameters, since baryonic cross sections are larger than mesonic ones and thus delay freeze-out [67]. In contrast, larger flow or temperature gradients tend to decrease the HBT radius parameters, since they narrow the spatial extension within which identical particle pairs show significant quantum-mechanical interference. The linear extrapolation $R_i \propto (dN_{\text{ch}}/d\eta)^{1/3}$ provides an agnostic baseline on top of which dynamical changes may be established.

In models with flow-dominated freeze-out scenarios, the m_T -dependence of the transverse HBT radii steepens as flow increases and/or temperature decreases. However, the numerical significance of this effect is model-dependent and other factors (such as effects from resonance decay contributions or the opacity of the produced matter) may play a role as well. Even if one assumes that transverse flow effects increase with $\sqrt{s_{NN}}$ from RHIC to LHC, the question whether the m_T -dependence of transverse HBT radii steepens, appears to be too subtle to have a robust, model-independent answer. Moreover, in model studies, transverse flow may manifest itself in a K_T -dependence of transverse HBT radii, which cannot be absorbed in an m_T -dependence. We are not aware of sufficiently generic LHC predictions for this interesting class of measurements. As an aside, we note that for establishing the trend displayed in figure 5, data for different centralities and centre-of-mass energies should be compared at the *same* transverse momentum — otherwise, the strong m_T -dependence (4) may mask the apparently universal dependence on $(dN_{\text{ch}}/d\eta)^{1/3}$.

Under relatively mild model assumptions, the difference $R_o^2(K_T) - R_s^2(K_T)$ can be related to the lifetime of the particle-emitting source. The smallness of this quantity has been dubbed puzzling, since many models of the source dynamics predicted large lifetimes (for instance as a consequence of a first order phase transition or rapid crossover) [68]. Also, fluid dynamics strongly over-predicts $R_o^2 - R_s^2$, if it is not supplemented by extended hadronic scattering mechanisms [69], or by other significant modifications of the final state [70]. In the energy range from RHIC to LHC, no mechanism is expected to set in, which could modify the value $R_o^2(K_T) - R_s^2(K_T)$ significantly.

The analysis of femtoscopic information at LHC is not limited to the three generic features listed above. It includes the analysis of HBT radii with respect to the reaction plane [28], the physics hidden in the intercept parameter λ of equation (3), and a rapidly growing field of non-identical particle correlations. So far, however, data on these classes of observables are too scarce to serve as a robust baseline for extrapolations to the LHC, and we refer to a recent review article for further discussions [63].

7. Single inclusive high-pt spectra in A - A and pA collisions

The study of single inclusive hadron spectra at high transverse momentum has led to some of the major discoveries of the RHIC heavy ion program [71]. At the SPS, kinematic constraints limit the analysis of transverse momentum spectra in practice to $p_T \leq 3 - 4$ GeV/ c . In contrast, the RHIC program studied at higher centre-of-mass energy various hadron species in a range up to $p_T \leq 10 - 20$ GeV/ c , where perturbative production mechanisms are known to account for the single inclusive spectra in hadronic collisions. At the LHC, the transverse phase space accessible for such measurements increases by another factor ~ 10 . The limited kinematic reach of the SPS prompts us in the following sections to base extrapolations to the LHC on RHIC data only.

The nuclear modification factor R_{AB}^h characterizes how the production of a hadron h in a nucleus-nucleus collisions A - B differs from its production in an equivalent number of proton-proton collisions,

$$R_{AB}^h(p_T, \eta, \text{centrality}) = \frac{\frac{dN_{\text{medium}}^{AB \rightarrow h}}{dp_T d\eta}}{\langle N_{\text{coll}}^{AB} \rangle \frac{dN_{\text{vacuum}}^{pp \rightarrow h}}{dp_T d\eta}}. \quad (5)$$

Here, $\langle N_{\text{coll}}^{AB} \rangle$ is the average number of inelastic nucleon-nucleon collisions in a given centrality class. This number is typically determined in a Glauber-type calculation. The nuclear modification factor depends in general on the transverse momentum p_T and pseudo-rapidity η of the particle, the particle identity h , the centrality of the collision and the orientation of the particle trajectory with respect to the reaction plane (which is often averaged over). In the absence of medium effects, $R_{AB}^h = 1$.

7.1. The nuclear modification factor at mid-rapidity

RHIC data on R_{AA} show the following generic features:

- (i) Characteristic centrality dependence of R_{AA} and R_{dAu} .

For the most peripheral centrality bin, the nuclear modification factors measured at RHIC are consistent with the absence of medium-effects in both nucleus-nucleus ($R_{AA} \sim 1$) and deuterium-nucleus ($R_{dAu} \sim 1$) collisions [72–75]. With increasing centrality, R_{AA} decreases monotonically. In d-Au collisions, the opposite centrality dependence is observed with maximal values $R_{dAu} \sim 1.5$ around $p_T = 3 - 5$ GeV/ c in the most central bin. Accordingly, one observes that R_{AA} depends on the azimuth with respect to the reaction plane, with a smaller R_{AA} out-of-plane [76] — equivalently, $v_2(p_T)$ is positive at high p_T [36].

- (ii) Strong and apparently p_T -independent suppression of R_{AA} at high p_T .

In $\sqrt{s_{NN}} = 200$ GeV, 5-10% central Au-Au collisions at mid-rapidity, one observes a suppression of high- p_T single inclusive hadron yields by a factor ~ 5 , corresponding to $R_{AuAu}^h(p_T) \simeq 0.2$ for $p_T \geq 5 - 7$ GeV/ c . Within experimental errors, this suppression is p_T -independent for higher transverse momenta in all centrality bins [77–79].

(iii) Independence of R_{AA} on hadron identity.

For transverse momenta $p_T \geq 5 - 7$ GeV/ c , all identified (light-flavoured) hadron spectra show a quantitatively comparable degree of suppression. There is no particle-species dependence of the suppression pattern at high p_T .

(iv) The photon spectrum is consistent with perturbative expectations.

For single inclusive photon spectra, the nuclear modification factor shows mild deviations from $R_{AuAu}^\gamma = 1$ [80]. Within errors, these are consistent with perturbative predictions taking into account the nuclear modifications of parton distribution functions (mainly the isospin difference between protons and nuclei) [81].

(v) R_{AA} shows a characteristic baryon-meson difference at intermediate p_T .

At intermediate p_T , 3 GeV/ $c < p_T < 6$ GeV/ c say, the nuclear modification factor for mesons is smaller than the one for baryons [82]. Within experimental uncertainties and irrespective of the hadron mass, all identified meson spectra show a similar degree of nuclear suppression, and so do all identified baryon spectra.

For hadronic collisions, the perturbative QCD factorized formalism can account systematically for single inclusive hadron spectra at sufficiently high transverse momentum, by convoluting (“incoming”) parton distribution functions, with hard, partonic scattering matrix elements, and with (“outgoing”) parton fragmentation functions. In nucleus-nucleus collisions, one aims at identifying the leading medium-length enhanced nuclear effects which modify this factorized formalism [83]. In this context, the notions “ingoing” and “outgoing” become physically relevant, since the hard production process is placed within the spatio-temporal geometry of a nuclear collision. The zeroth order question is whether the dominant medium modification is accumulated during the incoming or outgoing stage of its prolonged interaction with the medium. Experimentally, this can be addressed by systematically varying the final state effects; for instance by varying the outgoing in-medium path length via centrality measurements, or by switching off final state effects by comparing A - A collisions with hA collisions. Theory addresses these dependencies in model studies, which supplement the perturbative QCD factorization approach to single inclusive hadron spectra with medium-modifications in the initial and final state, taking the spatio-temporal distribution of matter during the A - A collision into account [84–86].

RHIC data prove that high- p_T hadron suppression is predominantly a final state effect by establishing that the suppression is not seen in d-Au and that it increases in A - A with increasing centrality and thus with increasing in-medium path length in the final state [point (i)]. Moreover, the independence of R_{AA}^h on hadron identity [point (ii)] at high p_T gives support to the picture that the final state medium modification of parton fragmentation is of partonic nature, i.e. that it occurs prior to the onset of hadronization. This is so, since hadronic states would present absorption cross sections which can be expected to differ significantly with hadron identity, and should thus lead to a hadron-specific splitting of the nuclear suppression factor R_{AA}^h , which is not observed

above $p_T \geq 5-7$ GeV/ c . In addition, the single inclusive photon spectrum indicates that initial state effects at high p_T are small and that they may be accounted for by nuclear modified parton distributions [point (iv)]. From these arguments, one concludes that the suppression of high- p_T single inclusive hadron spectra in nucleus-nucleus collisions is due to a *partonic, medium-length dependent final state effect*.

From an agnostic point of view, one wonders whether the generic features (i)-(v) persist at the 30 times higher $\sqrt{s_{NN}}$ explored at the LHC, and how these features evolve in the much wider transverse momentum range accessible at the LHC. To discuss these questions, we first turn in section 7.1.1 to the extrapolation of models that describe the generic features observed in RHIC data. Then, we provide in section 7.1.2 a list of effects that may become important at the LHC and could lead to characteristic deviations from the generic features observed at RHIC.

7.1.1. Extrapolations of parton energy loss models to the LHC. The generic features (i)-(iv) are naturally accommodated in models which supplement the perturbative QCD factorization approach (using nuclear parton distribution functions) with a mechanism which degrades the energy of the leading outgoing partonic fragment due to its propagation in matter. Two classes of mechanisms have been explored in Feynman diagrammatic detail: collisional [87] and radiative parton energy loss [88–92, 100]. Radiative energy loss, that is the medium-enhanced splitting of the energetic parton, is the dominant mechanism at high p_T [84–86]. Up to which p_T subleading collisional effects are numerically significant and how they could be disentangled from radiative ones is a matter of ongoing debate [93–95]. In the following, we limit our considerations to radiative energy loss, which gives a fair description of RHIC data above $p_T > 7$ GeV/ c [96–99]. This may provide a baseline on top of which collisional contributions can be established.

In radiative parton energy loss models, only one medium-dependent model parameter enters, the so-called jet quenching parameter $\hat{q}(\tau)$ (or a reparametrization of it), which depends on the time τ after the collision. In model studies, it is often expressed in terms of the energy density $\epsilon(\tau)$ [100]

$$\hat{q}(\tau) = c \epsilon^{3/4}(\tau), \quad (6)$$

where c is assumed to be a time- and temperature-independent constant. An estimate based on perturbatively weak interactions between the hard parton and the medium gives $c \approx 2$ [101]. In contrast, fitting parton energy loss models to RHIC data, several groups found much larger values, $c \geq 8$ [98, 99, 102]. Assuming a 1-dimensional Bjorken expansion of the produced matter with $\hat{q}(\tau) = \hat{q}_0 \tau_0 / \tau$, this translates into a value*

$$\hat{q}(\tau = 1 \text{ fm}/c) \geq 4 \text{ GeV}^2/\text{fm}. \quad (7)$$

* Since medium-induced gluon energy radiation in an expanding medium depends on the line-average $\bar{\hat{q}} = \frac{2}{L^2} \int_0^L d\tau \tau \hat{q}(\tau)$ [103], several model studies quote $\bar{\hat{q}}$ for an average in-medium path length [98, 99]. However, $\bar{\hat{q}}$ depends strongly on L , which differs for each parton. This introduces additional uncertainties. To bypass these problems, we quote here the value c , or equivalently $\hat{q}(\tau = 1 \text{ fm}/c)$ which can be unambiguously extracted from all studies quoting $\bar{\hat{q}}$.

The precise value of \hat{q} consistent with RHIC data is currently debated, but it is generally thought that \hat{q} is significantly larger than the perturbative estimate $c = 2$ in reference [101].

The jet quenching parameter \hat{q} has a rigorous field theoretical definition in terms of the short-distance behaviour of the target expectation value of a light-like Wilson loop [104]. For a class of non-Abelian thermal gauge field theories, which are known to have a gravity dual, non-perturbative evaluations of \hat{q} have established recently that the seemingly small scale of an initial temperature of $T(\tau = 1 \text{ fm}/c) \simeq 300 \text{ MeV}$ does indeed give rise to a jet quenching parameter $\hat{q}(\tau = 1 \text{ fm}/c)$ numerically consistent with the apparently large lower bound of equation (7) [104]. These studies also show that the ratio of jet quenching parameters \hat{q} of different thermal field theories is determined by the square root of the ratio of their entropy densities [105]. In earlier studies, \hat{q} was taken to be proportional to the event multiplicity, and large values up to $\bar{\hat{q}}_{\text{LHC}} \simeq 7 \bar{\hat{q}}_{\text{RHIC}}$ were explored [98, 99]. On the other hand, the multiplicity extrapolations to the LHC shown in figure 1 would indicate a much smaller value of $\bar{\hat{q}}_{\text{LHC}}$, and — given that a multiplicity scaling of \hat{q} is an additional model assumption — a very mild increase of say $\hat{q}_{\text{LHC}} \simeq 1.25 \hat{q}_{\text{RHIC}}$ is conceivable. Since \hat{q} is the only medium-sensitive parameter in a class of model studies, once its value is fixed we can detail the predictions of these energy loss models for the LHC:

(i) Centrality dependence.

Parton energy loss models that implement final state effects only, predict the absence of nuclear suppression in the most peripheral collisions. As a consequence, one expects that the centrality dependence of R_{PbPb} at the LHC parallels the one observed at RHIC.

(ii) p_T -dependence of R_{PbPb} at the LHC.

At RHIC energies, the slope of the partonic p_T -spectrum gradually steepens as one moves from $p_T \sim 10 \text{ GeV}/c$ to the absolute kinematic boundary $p_T = 100 \text{ GeV}/c$. This implies that to obtain the same value of R_{AA} at higher p_T , a smaller fraction of parton energy loss is needed (“trigger bias effect”, see reference [96]). In contrast, at the LHC, the partonic p_T -spectrum will show almost the same power-law over the entire range $10 \text{ GeV}/c < p_T < 100 \text{ GeV}/c$, since this p_T -range is far away from the kinematic boundary at the LHC. This implies that for a p_T -independent $R_{AA}(p_T)$, one requires a constant, p_T -independent fractional energy loss, not predicted in current energy loss models [99]. For a mild increase of e.g. $\hat{q}_{\text{LHC}} \simeq 1.25 \hat{q}_{\text{RHIC}}$, models thus indicate that for central collisions, $R_{\text{PbPb}}(10 \text{ GeV}/c < p_T < 20 \text{ GeV}/c)$ is the same or slightly larger (by up to ~ 0.1) than at RHIC, and that $R_{\text{PbPb}}(p_T)$ increases gently by $0.1 - 0.2$ from $p_T = 10 \text{ GeV}/c$ to $p_T \sim 100 \text{ GeV}/c$ ‡.

‡ In this kinematic range, the partonic spectrum at the LHC is gluon dominated, while it is strongly quark dominated at RHIC. This difference in composition decreases the nuclear modification factor at LHC, compared to the one at RHIC, and compensates partially, but not completely for the trigger bias effect.

(iii) Dependence of R_{PbPb} on hadron identity.

Light-flavoured hadron spectra are expected to show the same nuclear suppression independent of hadron species at sufficiently high $p_T > p_T^{\text{pid}}$. If the particle species dependence at intermediate $p_T < p_T^{\text{pid}}$ is due to a medium-dependent hadronization mechanism (such as proposed for instance in recombination models [106–110]), then $p_T^{\text{pid}}(\sqrt{s_{NN}})$ is expected to increase with $\sqrt{s_{NN}}$ by up to 2 – 3 GeV/ c from RHIC to the LHC [110]. In contrast, if the scale p_T^{pid} is mainly set by the time dilation of the hadronization time [111], implying that for $p_T > p_T^{\text{pid}}$ hadronization occurs outside the medium, then one may expect that p_T^{pid} is $\sqrt{s_{NN}}$ -independent. Thus, the $\sqrt{s_{NN}}$ -dependence of p_T^{pid} may provide complementary information about the mechanism underlying the anomalous baryon-to-meson ratio at intermediate p_T .

For heavy-flavoured hadrons, parton energy loss models predict a hierarchy in the nuclear suppression [112–115], which can be characterized by “heavy-to-light” ratios of the corresponding nuclear modification factors of heavy-flavoured over light-flavoured hadrons [116]. For D -mesons, the charm mass is expected to be too small to contribute to a mass-dependent suppression above $p_T > 10$ GeV/ c . However, since light-flavoured hadrons at the LHC are dominated by gluon parents, the heavy-to-light ratio of D -mesons is sensitive to the colour charge dependence of parton energy loss and is expected to exceed unity by up to a factor ~ 1.5 in an extended p_T -range. In contrast, for B -mesons, the mass effect is expected to put strong limits on medium-induced energy loss in an extended p_T -range. The resulting heavy-to-light ratios are expected to be significantly larger than for D -mesons, reaching a factor $\sim 2 - 4$, even for relatively low estimates of the value of \hat{q} [116].

(iv) Single inclusive photon spectra.

Based on a naive extrapolation from RHIC data, one may expect that photon spectra deviate only mildly from $R_{AA}^\gamma \sim 1$ at the LHC. However, current parton energy loss models allow for mechanisms which may lead to significant medium-modifications: The medium-induced photon bremsstrahlung of hard partons may enhance the photon yield at high p_T [117]; hard partons, which fragment into photons, may reduce the photon yield at high p_T [118]. Both effects are of order α_{em} , and it is unknown to what extent they cancel each other and how they may vary as a function of p_T^γ .

7.1.2. Testing effects not encoded in current parton energy loss models. We now turn to phenomena that are qualitatively novel in the sense that they are not encoded in current parton energy loss models tested at RHIC, but may become important at the LHC.

- Is high- p_T hadron suppression at mid-rapidity a final state effect at all $\sqrt{s_{NN}}$? At RHIC, the absence of suppression in R_{dAu} showed conclusively, that initial state effects are unimportant for R_{AA} [72–75]. However, high- p_T suppression in pA has

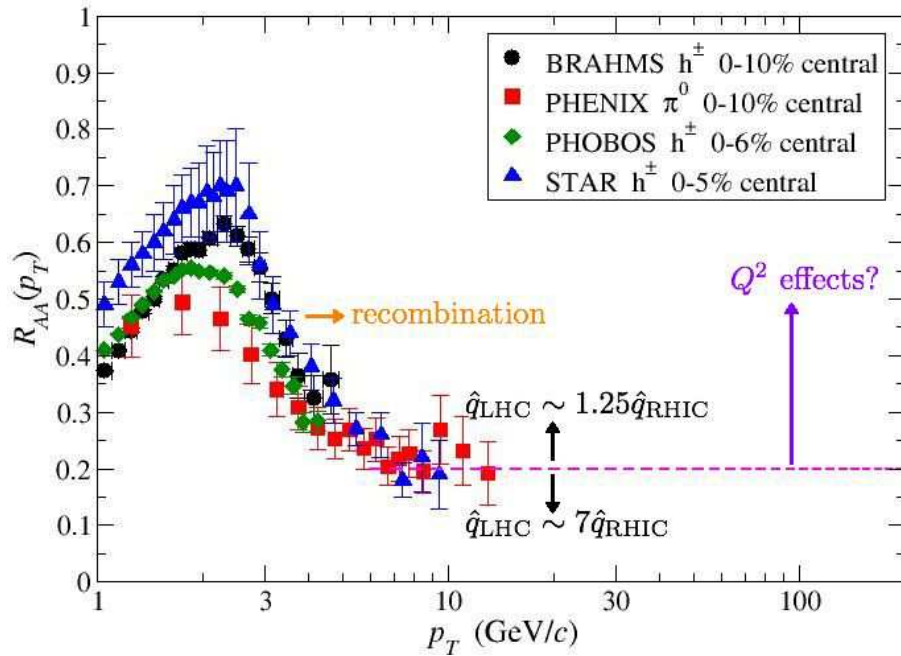


Figure 6. The nuclear modification factor R_{AA} as a function of transverse momentum at mid-rapidity. Data are for hadronic spectra measured at RHIC in $\sqrt{s_{NN}} = 200$ GeV Au-Au collisions. The dashed line is a straight continuation of the high- p_T trend at RHIC, reproduced by models of radiative parton energy loss. Arrows indicate qualitative tendencies of how R_{AA} may change at the LHC, see text for detailed discussion.

been predicted for sufficiently high $\sqrt{s_{NN}}$ as a consequence of non-linear QCD evolution in the so-called geometric scaling window [119–123]. At present, the value of $\sqrt{s_{NN}}$ at which non-linear evolution starts to become relevant for particle production at intermediate p_T is unclear. If the onset of such non-linear evolution effects should lie below LHC energy, then this would be signalled by $R_{pPb} < 1$ at LHC mid-rapidity. The enhancement $R_{dAu} > 1$ observed at RHIC mid-rapidity would turn into a characteristic suppression as a function of $\sqrt{s_{NN}}$. Moreover, one expects in this case that the nuclear modification factor in Pb-Pb will be suppressed due to both, initial and final state effects.

- Does $R_{PbPb}(p_T)$ show indications of medium-dependent Q^2 -evolution?

QCD evolution underlies the partonic fragmentation process in the perturbative regime, as well as the scale dependence of fragmentation functions. The question of how the medium affects the QCD scale evolution is difficult to address theoretically, since medium effects are “higher twist”, i.e. subleading by powers of Q^2 , although they may be nuclear enhanced by geometric factors $\propto A^{1/3}$ [124, 125]. Qualitatively, however, one may expect that — despite the time dilation of the parton fragmentation process in the target rest frame — at sufficiently large Q^2 , parton splitting occurs on length scales too short to be resolved by the medium, and short-distance contributions to parton fragmentation remain

unmodified accordingly. It has been speculated that this may lead to a significant rise of $R_{AA}(p_T)$ in the range $20 \text{ GeV}/c < p_T < 100 \text{ GeV}/c$ [126], but detailed model studies are still missing. More generally, the fact that LHC has access to a logarithmically wide p_T -range may provide novel opportunities to test the medium dependence of QCD-evolution.

- What is the dynamical mechanism underlying the nuclear modification of quarkonium?

Data on $R_{AA}^{J/\Psi}(p_T, \eta)$ at RHIC are known up to less than $p_T < 5 \text{ GeV}/c$. They indicate suppression at small p_T , $R_{AA}^{J/\Psi}(p_T \lesssim 1 \text{ GeV}/c, |\eta| \lesssim 0.35) \simeq 0.3 - 0.4$, and possibly an increase of $R_{AA}^{J/\Psi}$ with p_T . This is qualitatively similar to R_{AA}^h of light hadrons. However, the physics invoked to account for the suppression of J/Ψ 's shows marked differences if compared to the high- p_T suppression of light hadrons. Quarkonium suppression arises from the fact that the attraction between heavy quarks and anti-quarks weakens with increasing temperature due to dynamic screening effects [127]. According to recent models, directly produced J/Ψ 's may not dissociate until well above the energy densities attained at RHIC, but the χ_c 's and Ψ 's, whose decay contributions are estimated to $\sim 60\%$ of the J/Ψ yield in hadronic collisions, are expected to dissociate. The observed value $R_{AA}^{J/\Psi}(p_T < 1 \text{ GeV}/c, |\eta| < 0.35) \simeq 0.3 - 0.4$ thus appears natural, if one assumes that all excited $c\bar{c}$ bound states are dissociated in the medium [128, 129].

At the LHC, one will have for the first time experimental access to significant rates of both bound charmonium and bottomium states. The lowest lying $b\bar{b}$ -states are more tightly bound than the charmonium states, and one thus expects that they dissociate at higher temperature. Accordingly, in dissociation models one expects quite generally that the nuclear suppression of these bottomium yields is smaller or at most as large as that of the corresponding charmonium yields. A qualitatively opposite behaviour can be expected, if secondary production mechanisms, such as recombination, start playing a role [23]. These become more effective with the number of heavy quarks produced, and are thus more efficient in enhancing charmonium bound states.

At high transverse momentum, $p_T > 5 - 7 \text{ GeV}/c$, recombination effects are absent, and LHC will establish how the high- p_T modification of the spectra of mesonic $Q\bar{Q}$ bound states differs from that of heavy-light and light-light flavoured mesons. The following qualitative considerations illustrate the importance of formation time effects in this context: i) If high- p_T J/Ψ 's originate from gluon parents and if these gluons propagate over long distances before hadronizing, then the nuclear modification factor of J/Ψ 's is expected to be reduced due to gluon energy loss, and should take the same value as that for light-flavoured hadrons. ii) In contrast, if high- p_T J/Ψ 's would originate from the fragmentation of c -quark parents and if the quark propagates over long distances prior to hadronizing, then the nuclear modification factor is expected to be reduced due to quark energy loss only, and should match the smaller reduction of heavy-light flavoured hadrons $R_{AA}^{J/\Psi} \simeq R_{AA}^D >$

R_{AA}^h . In this case, one would also expect in pp collisions open charm production associated with J/Ψ production. iii) If in contrast the formation time of the J/Ψ is small compared to the extension of the collision region ~ 10 fm, then it is a $Q\bar{Q}$ bound state of velocity v increasing with p_T , which propagates through the medium. For this case, non-perturbative calculations based on the AdS/CFT correspondence suggest that the screening length L_s of the $Q\bar{Q}$ potential at temperature T shows a characteristic velocity scaling $L_s(v, T) \propto L_s(0, T)/\sqrt{\gamma}$ [130]. Model estimates indicate that depending on the binding energy of the $Q\bar{Q}$ -state, it is this velocity-dependent dissociation effect which may dominate in an extended intermediate p_T -regime. Only in this latter case will different bound states such as J/Ψ and Ψ' show a different degree of suppression.

- Are high- p_T single inclusive photon spectra sensitive to final state medium effects? In hadronic collisions at the LHC, a significant fraction of the single inclusive photons arises from the fragmentation of quarks and (at next-to-leading order) gluons. If the parent partons suffer medium-induced energy degradation prior to fragmenting into a photon [118], then R_{AA}^γ is reduced and the elliptic flow of photons receives a positive contribution [131, 132]. The strength of this effect may allow one to constrain the photon formation time but is difficult to estimate a priori. On the other hand, the interaction of the produced partons with the medium can lead to additional bremsstrahlung photons [117]. This effect increases R_{AA}^γ , and contributes to a negative v_2 for photons [132]. To the best of our knowledge, these expectations remain qualitative to date, but the wider kinematic reach at LHC should help to disentangle them in the data. We finally note that similar modifications of the high- p_T spectrum are not expected for Z -bosons, since all aspects of its production are local and unlikely to interfere with the typical length and momentum scales present in the produced QCD matter.

7.2. The nuclear modification factor as a function of rapidity.

7.2.1. *Evolution of the Cronin peak at RHIC.* The notion ‘‘Cronin peak’’ refers to the enhancement of the nuclear modification factor R_{hA} above unity at intermediate transverse moment, $2 \text{ GeV}/c \lesssim p_T \lesssim 4 \text{ GeV}/c$. At lower transverse momentum, the nuclear modification factor is generally suppressed $R_{hA} < 1$. We hasten to remark that the notion ‘‘Cronin peak’’ is but a description and not an explanation of the shape of R_{hA} . As discussed below, there is no completely satisfactory explanation of the dynamical origin of the Cronin peak so far, but LHC is well-positioned to provide additional insight.

The kinematically available p_T -range decreases with increasing rapidity, and data from RHIC are currently limited to $p_T < 5 \text{ GeV}/c$ for $|\eta| > 2$. Within this limited range, one observes the following apparently generic trends in RHIC data [133]:

- (i) Rapidity and p_T -dependence of R_{dAu} .

At RHIC, R_{dAu} shows a typical Cronin enhancement for $\eta \leq 1$. This Cronin peak in the range $2 \text{ GeV}/c \leq p_T \leq 4 \text{ GeV}/c$ monotonically decreases in the deuteron fragmentation region. One finds $R_{\text{dAu}} \simeq 1$ at $\eta \simeq 1$, $R_{\text{dAu}} \simeq 0.5$ at $\eta = 3$ [134–136] and even smaller values for π^0 's at higher rapidity [137]. In contrast, in the nucleus fragmentation region, the ratio R_{cp} of central over an equivalent number of peripheral collisions, which is closely related to R_{dAu} , shows an enhancement [136] above unity, which increases with increasing rapidity.

(ii) Centrality dependence of suppression pattern in d-Au.

At mid-rapidity, R_{cp} increases around the Cronin peak for increasing centrality. In contrast, the centrality dependence at forward deuteron rapidity is inverted [136]: R_{dAu} decreases with increasing centrality for $\eta > 1$, and the centrality dependence at $\eta \simeq 1$ is negligible.

In the context of RHIC data, the discussion of these phenomena has focused on two initial state effects, which we address now: multiple scattering and non-linear QCD evolution of the incoming parton distribution functions.

The Cronin peak is often thought of as the consequence of a multiple scattering picture, in which the partons in the deuteron wavefunction undergo multiple interactions in the target nucleus prior to producing relatively high- p_T hadrons. Incoherent multiple scattering of these incoming partons leads to a transverse momentum broadening of the initial parton distribution, which translates into a correspondingly broadened single inclusive hadron spectrum. This can account for the observed Cronin peak at mid-rapidity [138, 139], though it is unclear whether it can account for the particle species dependence of the effect. Moreover, at least in their current model implementations, such multiple scattering models predict the persistence of the Cronin peak at forward rapidity, and they imply an increase of p_T -broadening with increasing centrality at all rapidities [138]. This contradicts the generic trends seen in the RHIC data.

In studies of non-linear QCD evolution at small momentum fractions x , one generically finds that the growth of unintegrated gluon distribution functions with $\ln 1/x$ (or with $\ln \sqrt{s_{NN}}$) is saturated up to a scale $p_T < Q_s(x)$, which grows with $1/x$. Moreover, above this saturation scale, non-linear QCD evolution characteristically changes the power-law in a wide geometric scaling window. Contact between these findings and the phenomenology of d-Au collisions is made by the following observations: First, toward deuteron projectile rapidity, smaller momentum fractions x_{Au} of the nuclear parton distribution functions become relevant for particle production. Eventually, x_{Au} will become small enough for non-linear QCD evolution to be applicable. Second, convoluting non-linear evolved unintegrated nuclear parton distributions schematically with hard processes, one finds that non-linear QCD evolution implies the decrease of R_{hA} with increasing $\ln 1/x_{\text{Au}}$ [119–123]. This provides a conceivable explanation for the rapidity dependence of R_{dAu} .

Non-linear QCD evolution does not account for all trends seen in the data. In particular, the Cronin peak itself is not a dynamical consequence of non-linear QCD

evolution, it is just a conceivable initial condition, which is quickly washed out by the evolution. So, if saturation physics is the correct explanation for the rapidity dependence of R_{dAu} , then one knows that it is not applicable at RHIC mid-rapidity. Also, while particle species identified data on R_{dAu} are not accurate enough to allow for decisive tests, the question whether a purely partonic explanation is sufficient to account for R_{dAu} in the experimentally tested range remained open so far. Moreover, it is unclear on theoretical grounds whether saturation physics can be expected to apply for the relatively large values $x_{\text{Au}} \geq 0.02$ [140] which dominate forward particle production at RHIC.

Experiments at the LHC will allow us to compare the $\sqrt{s_{NN}}$ - and η -dependence. To illustrate that this may provide a decisive test for current models, let us consider an alternative explanation of the rapidity dependence of R_{dAu} at RHIC, based on the following picture: Partons in the deuteron wave function undergo *inelastic* multiple scatterings on the nuclear target field. Hence, these partons split due to interactions with the target. Since splitting is very effective in energy degradation, this will deplete the hadron yield at forward rapidity but will enhance it at mid-rapidity. Also, the opposite centrality dependence at mid-rapidity and forward rapidity [point (ii)] can be understood in this way. In this picture, the suppression in R_{dAu} increases strongly with increasing projectile rapidity, because the energy degradation occurs on top of an increasingly steeply falling spectrum at forward rapidity. Transverse momentum broadening could still contribute to the Cronin peak at mid-rapidity, but would not be able to overcome the reduction at forward rapidity. This picture accounts for the same rapidity dependence as saturation models. In contrast to saturation models, however, it implies that the Cronin peak will not disappear with increasing $\sqrt{s_{NN}}$, but will persist at LHC energies.

7.2.2. Conceivable effects on the η -dependence of R_{pPb} and R_{PbPb} at the LHC. The example given above illustrates that comparing the $\sqrt{s_{NN}}$ - and η -dependence at the LHC will provide a qualitatively novel test for the saturation physics interpretations of measurements at RHIC. This is so, since an increase in both $\sqrt{s_{NN}}$ or η gives access to smaller momentum fractions x in the parton distributions, and thus has similar implications in saturation models. At the LHC, the $\sqrt{s_{NN}}$ -dependence of measurements, in combination with their η -dependence, will become a tool to discriminate effects from small- x QCD evolution from other conceivable mechanisms.

Focusing in the following solely on the nuclear modification factor, we now list phenomena which may affect significantly the η -dependence of R_{PbPb} at the LHC, and which may be disentangled by studying the $\sqrt{s_{NN}}$ -dependence in a combination of data from RHIC and LHC. Our list starts with conceivable final-state effects:

- (i) Dependence of R_{PbPb} on $dN_{\text{ch}}/d\eta$ for fixed centrality.

As discussed in section 7.1.1, the quenching parameter \hat{q} is expected to grow monotonously with $dN_{\text{ch}}/d\eta$. So, the quenching parameter should be smaller at forward rapidity. This effect contributes to an *increase* of R_{PbPb} with η .

(ii) The η -dependence of the partonic p_T -spectrum.

With increasing η , partonic p_T -spectra get steeper. This is a simple kinematic effect, present both at RHIC and at the LHC, but quantitatively different. As a consequence of this effect, the same amount of parton energy loss leads to a *decrease* of R_{PbPb} with η (trigger bias).

(iii) Flow effects on R_{PbPb} .

The initial parton, produced in a hard collision, needs not be produced within longitudinal comoving matter. In case that it is not, there is a relative longitudinal velocity between the hard projectile and the medium, and energy loss is expected to be higher. This effect is likely to contribute to a *decrease* of R_{PbPb} with η [141,142], though estimates of its magnitude vary widely [143].

(iv) Initial state effects.

As discussed above, the nuclear modification of parton distribution functions is expected to affect R_{PbPb} . In particular, models based on non-linear small- x evolution predict [119–123] an additional *decrease* of R_{PbPb} with η . These models can be tested by comparing the $\sqrt{s_{NN}}$ - and η -dependences in p -Pb collisions.

8. “Jet-like” particle correlations and jets

The leading hadronic fragments of highly energetic parent partons, measured in single inclusive hadron spectra, are strongly modified at RHIC and they are expected to be strongly modified at the LHC. Any model of the dynamical mechanism underlying this medium modification has implications for the entire parton fragmentation pattern, and that is: jets and jet-like observables. Jet measurements in heavy ion collisions are sensitive to how high-energy partons are attenuated in matter and how they equilibrate kinetically and chemically. In turn, these medium-modifications of jet fragmentation characterize properties of the produced medium.

In general, parton fragmentation leads to multiplicity distributions with broad variances. As a consequence, any particle trigger used to select jet-like observables will bias significantly the fragmentation pattern. Even prior to invoking medium effects, such biases have dramatic consequences: In a typical single inclusive hadron spectrum (i.e. single particle trigger) at $p_T > 20$ GeV/ c , the hadrons will typically carry on average $\sim 3/4$ of the energy of their parent partons. In contrast, the leading hadron in a 100 GeV/ c jet, initiated by a light parton, carries typically only $\sim 1/4$ of the jet energy, simply because this jet fragmentation pattern is not biased by a single particle trigger. In the presence of a medium, additional “trigger biases” may arise. For instance, in the presence of strong final state energy loss, a high- p_T particle trigger will select particles produced mainly at the outskirts of the nuclear overlap region. The parent partons of these hadrons have had a particularly small in-medium path length and thus suffered particularly little parton energy loss (surface bias) [144]. Also, a high- p_T particle trigger will prefer events in which the initial state p_T -broadening effects move the dijet invariant mass towards the trigger. Thirdly, triggering on a high-energy hadron or requiring

a jet can lead to structures in the distribution of soft “background” particles, which are typically counted towards the medium, but which are related to the trigger and would not be found in minimum bias events. These general considerations prompt us to distinguish in the following discussion between “true” jets, jet-like particle correlations and soft structures causally related to high- p_T triggers.

8.1. The medium-modification of “true” jets

“True” jet measurements, that is measurements of the *entire* fragmentation pattern of high- E_T parent partons, have not been performed in heavy ion collisions so far. In the context of RHIC data, “jet quenching” refers to the suppression of single inclusive hadron spectra and high- p_T particle correlations. Yet, measurements at RHIC, as well as models of parton energy loss, give rise to a set of general expectations for “true” jet measurements in heavy ion collisions:

- (i) Longitudinal jet multiplicity distributions soften.
Parton energy loss, combined with energy-momentum conservation implies that the energy lost by the leading parton or hadron in the parton shower reappears in additional multiplicity of softer fragments. The entire longitudinal jet multiplicity distribution is expected to soften, and the total jet multiplicity is expected to increase, see e.g. references [126, 145].
- (ii) Transverse jet multiplicity distributions broaden.
Essentially all models of parton energy loss assume a significant transverse momentum transfer from the medium to the jet projectile. As a consequence, parton energy loss is generally thought to be accompanied by a broadening of the jet fragmentation pattern in the plane orthogonal to the jet axis [141, 142, 146, 147]. In case that the momentum transfer from the medium is asymmetric, for instance since the parton is embedded in a collective flow field, this jet broadening may show characteristic asymmetries [142, 146].
- (iii) The hadrochemical composition of jet fragments may be modified.
To date, most studies of jet medium-modifications focus on the longitudinal and transverse energy and multiplicity distributions. However, in current models of parton energy loss, the medium couples to the parton shower via gluon exchange, and thus alters the colour flow in the shower. This may be expected to affect the hadrochemical composition of the jet. Also, in principle, other quantum numbers such as baryon number or flavour may be exchanged between the medium and the jet [148].

We note that even if the *average* longitudinal jet multiplicity distribution softens, it may be possible that high- p_T triggered particle correlations remain insensitive to the properties of the medium. This is so, for instance, if the high- p_T trigger should select the subset of parton fragmentation patterns, that escaped with a negligible medium modification e.g. due to a surface bias effect. Similar remarks apply to the transverse jet multiplicity distribution and hadrochemical composition.

8.2. Jet-like particle correlations and a potential all-or-nothing mechanism

There is a class of measurements, in which a trigger hadron of high transverse momentum p_T^{trig} is correlated with associated hadrons as a function of their transverse momentum p_T^{assoc} and their azimuthal angle $\Delta\phi$ with respect to the trigger particle. We call such correlations “jet-like”, if p_T^{assoc} is relatively large, $2 \text{ GeV}/c < p_T^{\text{assoc}} < p_T^{\text{trig}}$, say. For a first theoretical work on jet-like correlations, see e.g. [149]. The generic trends seen in such correlation functions at RHIC are:

- (i) Near-side jet-like particle correlations in Au-Au are independent of centrality and similar to those in pp or d-Au.

In pp and Au-Au collisions at RHIC, near-side (i.e. small $\Delta\phi$) two-particle jet-like correlations show an enhancement characteristic of hard-scattering processes. Compared to pp collisions, the yield of high- p_T trigger particles decreases by a factor ~ 5 from peripheral to central Au-Au collisions at RHIC. In contrast, jet-like two-particle correlations do not show a significant centrality dependence. For sufficiently high threshold trigger $8 \text{ GeV}/c < p_T^{\text{trig}} < 15 \text{ GeV}/c$, the yield and $\Delta\phi$ -width of the near-side distribution is insensitive to the centrality of Au-Au collisions, and coincides with the measurement in d-Au collisions [150]. The same has been observed for lower trigger thresholds [151]. Also other features of jet-like p_T -triggered correlation functions, such as the ratio of like-sign to unlike-sign pairs in jet-like correlations [151], do not show any centrality dependence and are consistent with the data found in pp collisions.

- (ii) Back-side jet-like particle correlations decrease in yield with increasing centrality, but keep approximately the same width.

For intermediate p_T triggers ($4 \text{ GeV}/c < p_T^{\text{trig}} < 6 \text{ GeV}/c$) at RHIC, the associated particle yield for $p_T^{\text{assoc}} > 2 \text{ GeV}/c$ disappears as a function of centrality [151]. If one raises the trigger threshold to higher values ($8 \text{ GeV}/c < p_T^{\text{trig}} < 15 \text{ GeV}/c$), then the back-side jet-like structure reappears again, but the yield strongly decreases with centrality. The back-side structure shows no sign of azimuthal broadening [150,152].

The above features are qualitatively consistent with a schematic all-or-nothing mechanism, based on the following picture: If a hadron is triggered on with a high p_T^{trig} , then it is the leading fragment of a parton shower, which propagated essentially unperturbed through the medium (“complete survival of entire jet structure”). On the other hand, if the parton shower is significantly perturbed by the medium, then the energy of the leading fragment is degraded to such an extent, that it becomes unlikely to find this fragment in a high- p_T trigger bin (“no survival at all”). This all-or-nothing picture may be regarded as the most extreme form of a trigger bias: the trigger selects the subclass of unmodified parton fragmentation patterns and the medium-modification establishes itself solely in the reduced yield. In this way, this all-or-nothing picture accounts for the strongly reduced yield of high- p_T trigger particles, characterized e.g. by the nuclear modification factor, as well as for the suppression of the back-side yield. It can also account for the absence of broadening in both the near-side and the away-

side peaks by arguing that the particle pairs entering the jet-like correlation function belong to parton showers which escaped the medium essentially without interaction and thus without signs of medium-induced broadening. The picture is also qualitatively consistent with finer features seen in the data, such as the observation that for near-side correlations, the particle yield as a function of the effective fragmentation variable $z_T = p_T^{\text{assoc}}/p_T^{\text{trig}}$ is the same in d-Au and Au-Au, independent of centrality; on the away-side, the particle yield decreases with centrality but shows the same z_T -slope [152].

Can such an all-or-nothing mechanism be consistent with the dynamics of QCD radiation physics? To address this question, one may note first that for a steeply falling partonic p_T -distribution, it is conceivable that *all* high- p_T trigger bins are dominated by hadrons, whose parent partons suffered no medium-induced parton energy loss [96]. In other words: while hadrons, whose parents suffered some medium-induced energy loss must end up in some p_T -bin, they can — for steeply falling distributions — always be shifted to an abundantly populated lower p_T -bin, in which their yield is statistically negligible. Recent implementations of radiative parton energy loss can account at least qualitatively for this possibility by two features [98, 99, 102]: first, even for dense systems, recent models allow for a sizeable finite probability that the parton shower propagates unperturbed through the medium. Second, the distribution of leading fragments in the parton shower turns out to be very fragile, once the parton shower has interacted with the medium. In this way, current model implementations contain the main ingredients needed for implementing a strong surface bias, which may underlie the all-or-nothing mechanism sketched above. In model studies, one has also addressed more refined questions, such as whether the surviving yield in the away-side correlation arises predominantly from particle pairs emitted tangentially to the surface of the collision region [153, 154], so that neither the trigger nor the associated recoil particle traverses a significant amount of matter.

The all-or-nothing mechanism outlined here is a working hypothesis, which finds some support in RHIC data and current model analyses. If true, it is a dramatic illustration that jet-like particle correlations fall short of characterizing the distributions of quenched jets, simply because they trigger mainly on the small fraction of unquenched survivor jets. To refine this all-or-nothing mechanism (or rather: to replace it by a picture which allows for gradual manifestations of parton energy loss on jet-like correlations), one should study in particular correlations with lower p_T^{assoc} . This is so, since the trigger particle of p_T^{trig} , to the extent to which it does not arise from a medium-independent fragmentation, should be accompanied by an increased associated yield at sufficiently small p_T^{assoc} . At RHIC, lowering p_T^{assoc} below 2 GeV/ c for Au-Au collisions, one has observed indeed an enhanced associated yield with clear indications of broadening of the away-side peak. However, the kinematic range $p_T^{\text{assoc}} < 2$ GeV/ c is difficult to disentangle from the large underlying event multiplicity and it may be affected by other mechanisms, see section 8.3 below.

A trigger-biased class of jet measurements, which shows medium-modifications of associated jet multiplicity only below $p_T^{\text{assoc}} < 2$ GeV/ c , provides arguably only

limited access to a study of the entire quenched jet fragmentation — except, of course, if one could demonstrate that this trigger bias is unimportant and that these jet-like correlations are characteristic for the *average* medium-modified parton shower. The wider kinematic reach of heavy ion collisions at the LHC may provide means to this end. A jet of $E_T = 200$ GeV has on average ≈ 7 charged hadrons with $p_T^{\text{assoc}} > 5$ GeV/ c . Although jet-like correlations based on single trigger particles will bias significantly the average jet fragmentation pattern, one expects qualitatively that the distribution of associated particles should show imprints of medium-modifications (namely signs of p_T -broadening and enhanced yield) in a wider range of p_T^{assoc} , which can be disentangled more clearly from the underlying event multiplicity. However, this qualitative expectation is not yet supported by model studies.

8.3. The pedestal, the ridge, the Mach cone and all that ...

High- p_T triggers affect the underlying event in hadronic collisions. For instance, in comparison to minimum bias data, triggering on a high- p_T hadron in a pp collision increases the soft event multiplicity by a factor of order $\simeq 2$. The hard parton sits on top of a “pedestal”, which is wide in rapidity [155]. Within perturbation theory, such a pedestal may be expected, since large Q^2 -processes are accompanied by initial state radiation, which is broad in rapidity and which will manifest itself in additional low- p_T hadrons. Since this initial state radiation moves over long ranges with the beam fragments, non-perturbative physics may play an important role as well. Also, multiple parton interactions may contribute to the pedestal effect [156].

The pedestal observed in high- p_T -triggered hadron collisions is the prototype of a phenomenon, which is clearly related to the presence of a high- Q^2 process, but which is not due to final state parton fragmentation. As such, the pedestal is a structure in the low- p_T trigger-associated particle yield, which one cannot expect to reproduce in a model that superimposes a high- p_T final state fragmentation pattern on the multiplicity distribution of a minimum bias event. The state of the art of modelling high- p_T phenomena in heavy ion collisions is of the latter type, and one wonders whether there are — like the pedestal in pp — characteristic features in heavy ion collisions, which one misses in models superimposing medium-modified hard processes on minimum bias soft background.

One candidate for such a feature is the “ridge”: a trigger particle is accompanied by additional associated hadronic activity in some range of intermediate p_T^{assoc} at the *near-side only*. This additional multiplicity is wide in rapidity but, unlike the pedestal, it is not balanced by a similar amount of activity in the same range of p_T^{assoc} on the away-side. This phenomenon may arise e.g. in a picture [157], in which the pedestal is embedded in a transverse flow field. Namely, triggering on a high- p_T particle, one selects an interaction point which will preferably lie away from the centre of the collision region towards the direction of the trigger p_T . At this point in the transverse plane, collective transverse flow is also expected to point in the direction of the trigger p_T .

So, any additional initial state hadronic activity, associated with this trigger, may be expected to be transported by transverse flow towards the near-side.

The above is but one, albeit speculative, illustration that if one aims at studying values of p_T^{assoc} comparable to those in the bulk multiplicity, the study of medium-modified jet measurements cannot be limited to the study of medium-modified final state parton fragmentation patterns on top of minimum bias events. For low p_T^{assoc} , it becomes difficult to establish which part of the additional hadronic activity emerges from the fragmentation and energy loss of a hard final state parton. We note that also the much-discussed, broad structures in the away-side correlations, which have been suggested to indicate the appearance of Mach cones, do not persist for higher p_T^{assoc} , but are only seen in a rather narrow range of low transverse momentum. Radial flow, anisotropic flow, initial state radiation and trigger bias effects may all affect characteristic features of associated particle distributions in this low p_T^{assoc} -regime. Heavy ion collisions at the LHC may help to clarify the dynamical understanding of such soft structures related to high- p_T trigger particles, since the hadronic activity in both the incoming and the outgoing state is expected to increase significantly with the trigger p_T , and may manifest itself in a wider range of p_T^{assoc} .

9. Connecting Heavy Ion Phenomenology with QCD

How collective phenomena emerge from the fundamental laws of elementary particle physics is a multi-faceted question, which in the range of extreme matter densities, where physics is determined by partonic degrees of freedom, has been addressed in different theoretical approaches. Historically, high-temperature QCD equilibrium dynamics, studied non-perturbatively in lattice calculations or perturbatively in finite temperature field theory, has been the first theoretical approach with the potential of connecting heavy ion phenomenology with first principles of QCD. In particular, the most dramatic collective phenomenon, expected in finite temperature QCD, namely the phase transition to a quark gluon plasma at a critical temperature and baryochemical potential, has been firmly established in lattice QCD. By now, these techniques are applied to many questions of phenomenological relevance at the LHC, including quarkonium suppression, the medium-modification of spectral functions, dissipative transport coefficients, and fluctuation measurements [158, 159].

On the other hand, heavy ion phenomenology has established over the last two decades strong indications that effects of directed collective motion are at least as important for understanding the dynamics of heavy ion collisions, than effects of random thermal motion. These two concepts, collective dynamics and local equilibrium, can coexist. Indeed, the modelling of heavy ion collisions in terms of perfect fluid dynamics illustrates the extent to which a mesoscopic system with extreme position-momentum gradients may still maintain local thermal equilibrium. In the discussion of this hydrodynamic modelling, the emphasis has shifted gradually from fundamental tests of QCD thermodynamics (namely whether the QCD phase

transition and its order leave traces in the dynamical evolution) to fundamental tests of QCD hydrodynamics (namely the test of dissipative properties of the matter, such as viscosities). There are many reasons for this gradual shift of focus at collider energies, starting with the observation that at RHIC and LHC energies one likely overshoots the critical energy density significantly, and ending with the notorious problem of identifying “unambiguous” signatures of the QCD phase transition. In principle, the characterization of hydrodynamic features in heavy ion collisions provides an opportunity of connecting heavy ion phenomenology to first principles in QCD, since both properties of the QCD phase transition and dissipative transport coefficients are calculable directly from the QCD Lagrangian. In practice, however, one prerequisite for exploiting these opportunities is a very good experimental and theoretical control over the “perfect fluid baseline” on top of which one aims at establishing dissipative properties. Our discussion in sections 3, 5 and 6 also identified how measurements at the LHC can help to establish whether conditions close to this perfect fluid baseline are realized at the LHC *and* whether they were realized at RHIC.

It would be an unwanted bias to limit the study of “soft” physics at the LHC to manifestations of QCD thermo- and hydrodynamics. In this review, we deliberately started from the observation that several apparently generic trends in the existing data (e.g. in multiplicity distributions and collective flow) have not yet found a satisfactory explanation. Agnostic extrapolations of these trends to the LHC are at odds with the extrapolation of current models, be it hydrodynamics or saturation physics. This indicates that LHC will be a discovery machine also in the soft physics sector. In particular, the support for an interpretation of data in terms of hydrodynamics or saturation physics would be strengthened qualitatively, if one discovered at the LHC deviations from the so far apparently generic trends, which are characteristic for the currently advocated dynamical models (such as a mild but distinct power-law $\sqrt{s_{NN}}$ increase of event multiplicity, or a deviation of v_2 from $\ln \sqrt{s_{NN}}$ -scaling). On the other hand, a confirmation of these trends may prompt us to reassess our understanding of the soft matter produced in heavy ion collisions at both LHC *and* RHIC.

LHC will also be a discovery machine outside the soft physics sector at mid-rapidity. This is so mainly because of the logarithmically wide range in transverse and longitudinal momentum, which opens up at 30 times higher $\sqrt{s_{NN}} = 5.5$ TeV. As discussed in sections 7 and 8, the resulting abundance of hard processes at the LHC provides many novel tools for probing the produced soft matter. The prerequisite for exploiting this opportunity is a very good experimental and theoretical control over how the medium modifies hard processes due to interactions in the final and initial state. Our discussion in section 8 identified how measurements at the LHC can improve this control, in particular by extending jet quenching studies significantly beyond the analysis of medium-modified leading fragments. This is likely to refine our understanding of hard probes at the LHC *and* at RHIC.

It would be an unwanted bias to limit the study of hard physics at the LHC to its use as “hard probes”. With the significantly wider kinematic reach, heavy ion physics gains

experimental access to other fundamental properties of QCD. In particular, medium modifications of the QCD-evolution in both Q^2 (mainly via the transverse momentum dependence) and $\ln 1/x$ (mainly via the rapidity and $\sqrt{s_{NN}}$ -dependence) become testable at the LHC. Again, characteristic deviations of LHC measurements from the agnostic extrapolations discussed here may provide some of the cleanest possibilities of identifying and ultimately quantifying the manifestations of medium-dependent QCD evolution.

References

- [1] Armesto N *et al* 2007 *Proceedings of the CERN TH Institute "Heavy Ion Collisions at the LHC — Last Call for Predictions"*, 14 May-8 June 2007, CERN, Geneva, to appear
- [2] Dokshitzer Yu L, Khoze V A and Troian S I 1992 *Z. Phys. C* **55** 107
- [3] Butterworth J M and Carli T 2004 *Preprint* hep-ph/0408061.
- [4] Eskola K J 2002 *Nucl. Phys. A* **698** 78
- [5] Armesto N and Pajares C 2000 *Int. J. Mod. Phys. A* **15** 2019
- [6] Busza W 2004 *Acta Phys. Polon. B* **35** 2873
- [7] Benecke J, Chou T T, Yang C N and Yen E 1969 *Phys. Rev.* **188** 2159
- [8] Back B B *et al* (PHOBOS Collaboration) 2003 *Phys. Rev. Lett.* **91** 052303
- [9] Back B B *et al* (PHOBOS Collaboration) 2006 *Phys. Rev. C* **74** 021901
- [10] Armesto N, Salgado C A and Wiedemann U A 2005 *Phys. Rev. Lett.* **94** 022002
- [11] Kharzeev K, Levin E and Nardi M 2005 *Nucl. Phys. A* **747** 609
- [12] Eskola K J, Kajantie K, Ruuskanen P V and Tuominen K 2000 *Nucl. Phys. B* **570** 379
- [13] Braun-Munzinger P, Redlich K and Stachel J 2004 *Quark Gluon Plasma 3* ed R C Hwa and X N Wang (Singapore: World Scientific) p 491
- [14] Andronic A, Braun-Munzinger P and Stachel J 2006 *Nucl. Phys. A* **772** 167
- [15] Cleymans J, Kraus I, Oeschler H, Redlich K and Wheaton S 2006 *Phys. Rev. C* **74** 034903
- [16] Wheaton S and Cleymans J 2004 *Preprint* hep-ph/0407174
- [17] Wheaton S and Cleymans J 2005 *J. Phys. G: Nucl. Part. Phys.* **31** S1069
- [18] Torrieri G, Jeon S, Letessier J and Rafelski J (2006) *Comput. Phys. Commun.* **175** 635
- [19] Letessier J and Rafelski J 2002 *Hadrons and quark-gluon plasma* (Cambridge: Cambridge University Press)
- [20] Andronic A, Braun-Munzinger P, Redlich K and Stachel J 2003 *Phys. Lett. B* **571** 36
- [21] Gazdzicki M and Gorenstein M I 1999 *Phys. Rev. Lett.* **83** 4009
- [22] Braun-Munzinger P, Stachel J and Wetterich C 2004 *Phys. Lett. B* **596** 61
- [23] Thews R L, Schroedter M and Rafelski J 2001 *Phys. Rev. C* **63** 054905
- [24] Rafelski J and Letessier J 2006 *Eur. Phys. J. C* **45** 61
- [25] Lee K S, Heinz U W and Schnedermann E 1990 *Z. Phys. C* **48** 525
- [26] Xu N and Kaneta M 2002 *Nucl. Phys. A* **698** 306c
- [27] Antinori F *et al* (NA57 Collaboration) 2004 *J. Phys. G: Nucl. Part. Phys.* **30** 823
- [28] Wiedemann U A and Heinz U W 1999 *Phys. Rept.* **319** 145
- [29] Retière F and Lisa M A 2004 *Phys. Rev. C* **70** 044907
- [30] Teaney D, Lauret J and Shuryak E V 2001 *Preprint* nucl-th/0110037
- [31] Kolb P F and Heinz U 2004 *Quark Gluon Plasma 3* ed R C Hwa and X N Wang (Singapore: World Scientific) p 634
- [32] Baier R, Romatschke P and Wiedemann U A 2006 *Phys. Rev. C* **73** 064903
- [33] Alessandro B *et al* (ALICE Collaboration) 2006 *J. Phys. G: Nucl. Part. Phys.* **32** 1295
- [34] Ollitrault J-Y 1992 *Phys. Rev. D* **46** 229
- [35] Back B B *et al* (PHOBOS Collaboration) 2005 *Phys. Rev. Lett.* **94** 122303
- [36] Adams J *et al* (STAR Collaboration) 2005 *Phys. Rev. C* **72** 014904
- [37] Snellings R 2004 *Heavy Ion Phys.* **21** 237

- [38] Adler S S *et al* (PHENIX Collaboration) 2005 *Phys. Rev. Lett.* **94** 232302
- [39] Voloshin S A 2003 *Nucl. Phys. A* **715** 379c
- [40] Heinz U W and Kolb P F 2004 *J. Phys. G: Nucl. Part. Phys.* **30** S1229
- [41] Bhalerao R S, Blaizot J-P, Borghini N and Ollitrault J-Y 2005 *Phys. Lett. B* **627** 49
- [42] Adare A *et al* (PHENIX Collaboration) 2007 *Phys. Rev. Lett.* **98** 162301
- [43] Teaney D 2003 *Phys. Rev. C* **68** 034913
- [44] Bureau G, Bleibel J, Fuchs C, Faessler A, Bravina L V and Zabrodin E E 2005 *Phys. Rev. C* **71** 054905
- [45] Lu Y *et al* 2006 *J. Phys. G: Nucl. Part. Phys.* **32** 1121
- [46] Borghini N and Ollitrault J-Y 2006 *Phys. Lett. B* **642** 227
- [47] Csanád M *et al* 2005 *Preprint* nucl-th/0512078
- [48] Moore G D and Teaney D 2005 *Phys. Rev. C* **71** 064904
- [49] Zhang B, Chen L W and Ko C M 2005 *Phys. Rev. C* **72** 024906
- [50] Lin Z-w and Molnár D 2003 *Phys. Rev. C* **68** 044901
- [51] van Hees H, Greco V and Rapp R 2006 *Phys. Rev. C* **73** 034913
- [52] Abelev B I *et al* (STAR Collaboration) 2007 *Preprint* nucl-ex/0701010
- [53] Alver B *et al* (PHOBOS Collaboration) 2007 *Preprint* nucl-ex/0702036
- [54] Bhalerao R S and Ollitrault J-Y 2006 *Phys. Lett. B* **641** 260
- [55] Adil A *et al* 2006 *Phys. Rev. C* **74** 044905
- [56] Lappi T and Venugopalan R (2006) *Phys. Rev. C* **74** 054905
- [57] Alt C *et al* (NA49 Collaboration) 2003 *Phys. Rev. C* **68** 034903
- [58] Roland G *et al* (PHOBOS Collaboration) 2006 *Nucl. Phys. A* **774** 113
- [59] Hirano T 2007 *Preprint* arXiv:0704.1699 [nucl-th]
- [60] Hirano T, Heinz U W, Kharzeev D, Lacey R and Nara Y 2006 *Phys. Lett. B* **636** 299
- [61] Back B B *et al* (PHOBOS Collaboration) 2005 *Phys. Rev. Lett.* **97** 012301
- [62] Adams J *et al.* (STAR Collaboration) 2004 *Phys. Rev. Lett.* **92** 062301
- [63] Lisa M A, Pratt S, Soltz R and Wiedemann U 2005 *Ann. Rev. Nucl. Part. Sci.* **55** 357
- [64] Chajęcki Z [STAR Collaboration] 2006 *AIP Conf. Proc.* **828** 566
- [65] Ferenc D, Heinz U V, Tomášik B, Wiedemann U A and Cramer J G 1999 *Phys. Lett. B* **457** 347
- [66] Sinyukov Yu M, Akkelin S V and Hama Y 2002 *Phys. Rev. Lett.* **89** 052301
- [67] Adamova D *et al* (CERES Collaboration) 2003 *Phys. Rev. Lett.* **90** 022301
- [68] Rischke D H and Gyulassy M 1996 *Nucl. Phys. A* **608** 479
- [69] Soff S, Bass S A and Dumitru A 2001 *Phys. Rev. Lett.* **86** 3981
- [70] Miller G A and Cramer J G 2007 *J. Phys. G: Nucl. Part. Phys.* **34** 703
- [71] Jacobs P and Wang X N 2005 *Prog. Part. Nucl. Phys.* **54** 443
- [72] Arsene I *et al* (BRAHMS Collaboration) 2003 *Phys. Rev. Lett.* **91** 072305
- [73] Adler S S *et al* (PHENIX Collaboration) 2003 *Phys. Rev. Lett.* **91** 072303
- [74] Back B B *et al* (PHOBOS Collaboration) 2003 *Phys. Rev. Lett.* **91** 072302
- [75] Adams J *et al* (STAR Collaboration) 2003 *Phys. Rev. Lett.* **91** 072304
- [76] Adler S S *et al* (PHENIX Collaboration) 2006 *Preprint* nucl-ex/0611007
- [77] Adams J *et al* (STAR Collaboration) 2003 *Phys. Rev. Lett.* **91** 172302
- [78] Back B B *et al* (PHOBOS Collaboration) 2005 *Phys. Rev. Lett.* **94** 082304
- [79] Adler S S *et al* (PHENIX Collaboration) 2006 *Phys. Rev. Lett.* **96** 202301
- [80] Isobe T *et al* (PHENIX Collaboration) 2007 *Preprint* nucl-ex/0701040
- [81] Arleo F 2006 *JHEP* **0609** 015
- [82] Abelev B I *et al* (STAR Collaboration) 2006 *Phys. Rev. Lett.* **97** 152301
- [83] Qiu J W 2005 *Eur. Phys. J. C* **43** 239
- [84] Baier R, Schiff D and Zakharov B G 2000 *Ann. Rev. Nucl. Part. Sci.* **50** 37
- [85] Kovner A and Wiedemann U A 2004 *Quark Gluon Plasma 3* ed R C Hwa and X N Wang (Singapore: World Scientific) p 192
- [86] Gyulassy M, Vitev I, Wang X N and Zhang B W 2004 *Quark Gluon Plasma 3* ed R C Hwa and

- X N Wang (Singapore: World Scientific) p 123
- [87] Bjorken J D 1982 *Preprint* FERMILAB-PUB-82-059-THY
 - [88] Gyulassy M and Wang X N 1994 *Nucl. Phys. B* **420** 583
 - [89] Zakharov B G 1997 *JETP Lett.* **65** 615
 - [90] Wiedemann U A 2000 *Nucl. Phys. B* **588** 303
 - [91] Gyulassy M, Lévai P and Vitev I 2001 *Nucl. Phys. B* **594** 371
 - [92] Wang X N and Guo X F 2001 *Nucl. Phys. A* **696** 788
 - [93] Adil A, Gyulassy M, Horowitz W A and Wicks S 2007 *Phys. Rev. C* **75** 044906
 - [94] Wang X N 2006 *Preprint* nucl-th/0604040
 - [95] Djordjevic M 2006 *Phys. Rev. C* **74** 064907
 - [96] Baier R, Dokshitzer Yu L, Mueller A H and Schiff D 2001 *JHEP* **0109** 033
 - [97] Vitev I and Gyulassy M 2002 *Phys. Rev. Lett.* **89** 252301
 - [98] Dainese A, Loizides C and Paic G 2005 *Eur. Phys. J. C* **38** 461
 - [99] Eskola K J, Honkanen H, Salgado C A and Wiedemann U A 2005 *Nucl. Phys. A* **747** 511
 - [100] Baier R, Dokshitzer Yu L, Mueller A H, Peigné S and Schiff D 1997 *Nucl. Phys. B* **484** 265
 - [101] Baier R 2003 *Nucl. Phys. A* **715** 209
 - [102] Renk T, Ruppert J, Nonaka C and Bass S A 2007 *Phys. Rev. C* **75** 031902
 - [103] Salgado C A and Wiedemann U A 2002 *Phys. Rev. Lett.* **89** 092303
 - [104] Liu H, Rajagopal K and Wiedemann U A 2006 *Phys. Rev. Lett.* **97** 182301
 - [105] Liu H, Rajagopal K and Wiedemann U A 2007 *JHEP* **0703** 066
 - [106] Molnár D and Voloshin S A 2003 *Phys. Rev. Lett.* **91** 092301
 - [107] Fries R J, Müller B, Nonaka C and Bass S A 2003 *Phys. Rev. Lett.* **90** 202303
 - [108] Greco V, Ko C M and Levai P 2003 *Phys. Rev. Lett.* **90** 202302
 - [109] Hwa R C and Yang C B 2003 *Phys. Rev. C* **67** 034902
 - [110] Fries R J, Müller B, Nonaka C and Bass S A 2003 *Phys. Rev. C* **68** 044902
 - [111] Wiedemann U A 2004 *J. Phys. G: Nucl. Part. Phys.* **30** S649
 - [112] Dokshitzer Yu L and Kharzeev D E 2001 *Phys. Lett. B* **519** 199
 - [113] Armesto N, Salgado C A and Wiedemann U A 2004 *Phys. Rev. D* **69** 114003
 - [114] Djordjevic M and Gyulassy M 2004 *Nucl. Phys. A* **733** 265
 - [115] Zhang B W, Wang E and Wang X N 2004 *Phys. Rev. Lett.* **93** 072301
 - [116] Armesto N, Dainese A, Salgado C A and Wiedemann U A 2005 *Phys. Rev. D* **71** 054027
 - [117] Zakharov B G 2004 *JETP Lett.* **80** 1 [*Pisma Zh. Eksp. Teor. Fiz.* **80** 3]
 - [118] Arleo F, Aurenche P, Belghobsi Z and Guillet J-P 2004 *JHEP* **0411** 009
 - [119] Kharzeev D, Levin E and McLerran L 2003 *Phys. Lett. B* **561** 93
 - [120] Baier R, Kovner A and Wiedemann U A 2003 *Phys. Rev. D* **68** 054009
 - [121] Albacete J L, Armesto N, Kovner A, Salgado C A and Wiedemann U A 2004 *Phys. Rev. Lett.* **92** 082001
 - [122] Kharzeev D, Kovchegov Yu V and Tuchin K 2003 *Phys. Rev. D* **68** 094013
 - [123] Jalilian-Marian J, Nara Y and Venugopalan R 2003 *Phys. Lett. B* **577** 54
 - [124] Luo M, Qiu J and Sterman G 1992 *Phys. Lett. B* **279** 377
 —1994 *Phys. Rev. D* **49** 4493
 —1994 *Phys. Rev. D* **50** 1951
 - [125] Guo X F and Wang X N 2000 *Phys. Rev. Lett.* **85** 3591
 - [126] Borghini N and Wiedemann U A 2005 *Preprint* hep-ph/0506218
 - [127] Matsui T and Satz H 1986 *Phys. Lett. B* **178** 416
 - [128] Karsch F, Kharzeev D and Satz H 2006 *Phys. Lett. B* **637** 75
 - [129] Satz H 2006 *J. Phys. G: Nucl. Part. Phys.* **32** R25
 - [130] Liu H, Rajagopal K and Wiedemann U A 2007 *Phys. Rev. Lett.* **98** 182301
 - [131] Fries R J, Müller B and Srivastava D K 2003 *Phys. Rev. Lett.* **90** 132301
 - [132] Turbide S, Gale C and Fries R J 2006 *Phys. Rev. Lett.* **96** 032303
 - [133] Debye R 2007 *Nucl. Phys. A* **785** 76

- [134] Arsene I *et al* (BRAHMS Collaboration) 2004 *Phys. Rev. Lett.* **93** 242303
- [135] Back B B *et al* (PHOBOS Collaboration) 2004 *Phys. Rev. C* **70** 061901
- [136] Adler S S *et al* (PHENIX Collaboration) 2005 **94** 082302
- [137] Adams J *et al* (STAR Collaboration) 2006 *Phys. Rev. Lett.* **97** 152302
- [138] Vitev I 2003 *Phys. Lett. B* **562** 36
- [139] Accardi A and Gyulassy M 2004 *Phys. Lett. B* **586** 244
- [140] Guzey V, Strikman M and Vogelsang W 2004 *Phys. Lett. B* **603** 173
- [141] Salgado C A and Wiedemann U A 2004 *Phys. Rev. Lett.* **93** 042301
- [142] Armesto N, Salgado C A and Wiedemann U A 2004 *Phys. Rev. Lett.* **93** 242301
- [143] Baier R, Mueller A H and Schiff D 2007 *Phys. Lett. B* **649** 147
- [144] Müller B 2003 *Phys. Rev. C* **67** 061901
- [145] Pal S and Pratt S *Phys. Lett. B* **574** 21
- [146] Armesto N, Salgado C A and Wiedemann U A 2004 *Preprint* hep-ph/0411341
- [147] Renk T and Ruppert J 2005 *Phys. Rev. C* **72** 044901
- [148] Sapeta S and Wiedemann U A 2007 *Preprint* in preparation
- [149] Majumder A and Wang X N 2005 *Phys. Rev. D* **70** 014007
- [150] Adams J *et al* (STAR Collaboration) 2006 *Phys. Rev. Lett.* **97** 162301
- [151] Adler C *et al* (STAR Collaboration) 2003 *Phys. Rev. Lett.* **90** 082302
- [152] Magestro D [STAR Collaboration] 2006 *Nucl. Phys. A* **774** 573
- [153] Renk T and Eskola K J 2007 *Phys. Rev. C* **75** 054910
- [154] Loizides C 2007 *Eur. Phys. J. C* **49** 339
- [155] Arnison G *et al* (UA1 Collaboration) 1983 *Phys. Lett. B* **132** 214
- [156] Sjöstrand T and van Zijl M 1987 *Phys. Rev. D* **36** 2019
- [157] Voloshin S A 2006 *Phys. Lett. B* **632** 490
- [158] Laermann E and Philipsen O 2003 *Ann. Rev. Nucl. Part. Sci.* **53** 163
- [159] Karsch F and Laermann E 2004 *Quark Gluon Plasma 3* ed R C Hwa and X N Wang (Singapore: World Scientific) p 1